DEGRADATION AND TREATMENT OF AZO REACTIVE DYES USING IRON OXIDE NANOPARTICLES

By

MUHAMMAD USAMA

SONIA LATIF

ZAINAB BALQEES

Department of Earth and Environmental Sciences
Bahria University, Islamabad

2016

DEGRADATION AND TREATMENT OF AZO REACTIVE DYES USING IRON OXIDE NANOPARTICLES

A thesis submitted to Bahria University, Islamabad in partial fulfilment of the requirement for the degree of BS in Environmental Sciences

MUHAMMAD USAMA

SONIA LATIF

ZAINAB BALQEES

Department of Earth and Environmental Sciences
Bahria University, Islamabad

2016

ABSTRACT

Industries are the major sources of pollution in all environments. Typical dyeing process, there are estimated 10-20% of dyes entering the environment through wastewater. Even a very low concentration of these dyes in water is undesirable. These effluents must be treated before they are released into the surrounding environment. Nanoparticles are becoming key components in a wide range of applications. In the present study 12gms of ferric chloride ($FeCl_3$) was dissolved in 150ml of distilled water and solution was vigorously stirred for 20mins to attain 3pH. Precipitation was achieved by adding 100ml solution of 2M NaOH dropwise under vigorous stirring. The final pH of solution was maintained 12. The prepared nanoparticles were then centrifuged at 1500rpm for 20mins. The pellets were than oven dried at $70^{O}C$ for 30mins. The dried iron oxide nanoparticles then grinded to attain a homogeneous size. Synthesised nanoparticles were characterised using Fourier Transform Infrared Spectroscopy (FTIR), Scanning Electron Microscopy (SEM) and X-rays Diffraction (XRD). There were three different dyes which are used for experiment i.e. Red, Yellow and Blue. To prepare a dye solutions, 100ml of tap water is mixed in 5% and 10% dyes to differ the concentration. Mix dye solution included 5% each dye in 100ml of tap water. Different pH dye solutions include pH 3, 5, 9 and 11. For acidic condition conc. HCl is used and for basic condition conc. NaOH is used. The results of characterization of synthesised nanoparticles shows the vibration at 3443.76 cm^{-1} and 1630.38 cm^{-1} in FTIR, SEM image showed the nanoparticles size range from 20nm to 80nm and XRD pattern analysis shows peaks at 2θ of 31.8596, 45.5656, 56.7600 and 75.3720. The crystalline average size was 53.83nm and of rhombohedral structure. After treatment of dyes with nanoparticles, experiment shows the significance decolourization and change in pH towards neutral phase.

ACKNOWLEDGEMENT

First, we would like to thank Allah Almighty, the most merciful and the most benevolent who guided us and helped us in our life and gave us the ability and power to carry out this study and bringing to end successfully. All respect and reverence for His Holy Prophet (SAW) who enabled us to shape our lives accordingly to the teaching of Islam.

We are thankful to our parents and siblings for their sustained moral and financial support. We are gratified by the help, support and encouragement provided by Dr. Tahseenullah Khan (HOD, E & ES, Bahria University) and our supervisor Syed Umair Ullah Jamil whose kind supervision and guidance enabled us to carry out this study with ease.

Special thanks and appreciation to Sir Imtiaz Khan who helped us in our entire lab related work and assisting us throughout this research.

ABBREVIATIONS

ADMI	American Dye Manufacturers Institute
BOD	Biological Oxygen Demand
COD	Chemical Oxygen Demand
DLS	Dynamic Light Scattering
EC	Electrical Conductivity
EDX	Energy Dispersive X-Ray Spectroscopy
ETAD	Ecological and Toxicological Association of the Dyestuffs
FTIR	Fourier Transform Infrared Spectroscopy
GT-FE NPs	Green Tea extracted Iron Nanoparticles
IONP	Iron Oxide Nanoparticles
JCPDS	Joint Committee on Powder Diffraction Standards
NPs	Nanoparticles
nZVI	Nano-scale Zero Valent Iron
SEM	Scanning Electron Microscopy
TDS	Total Dissolved Solids
USEPA	United States Environmental Protection Agency
UV	Ultraviolet
UV-Vis	Ultraviolet Visible
XRD	X-ray Diffraction

CONTENTS

		Page
ABSTRACT		i
ACKNOWLEDGEMENTS		ii
ABBREVIATIONS		iii
FIGURES		viii
TABLES		x
CHAPTER 1		
INTRODUCTION		
1.1	Nanoparticles	3
1.1.1	Iron Oxide Nanoparticles	4
1.1.2	Characterization of Iron Oxide Nanoparticles	5
1.1.2.1	Optical Properties of Iron Oxide NPs	5
1.1.3	Synthesis of Iron Oxide Nanoparticles	6
1.1.3.1	Iron Oxide NPs Thermal Decomposition Method	6
1.1.3.2	Iron Oxide NPs Co-Precipitation Method	7
1.2	Dyes	7
1.2.1	History of Dyes	7
1.2.2	Usage in Textile	8
1.2.3	Types	8
1.2.3.1	Acid Dyes	9
1.2.3.2	Basic Dyes	9
1.2.3.3	Direct Dyes	9
1.2.3.4	Fluorescent Dyes	9
1.2.3.5	Reactive Dyes	9
1.2.3.6	Sulphurous Dyes	10

1.2.3.7 Vat Dyes 10
1.2.3.8 Dye Precursors 10
1.2.3.9 Further Chemical Classification 10
1.3 Remediation 11
1.3.1 Physical Methods 11
1.3.2 Chemical Methods 11
1.3.3 Biological Methods 11
1.4 Remediation of Organic Compounds 11
1.5 Azo-Dyes 12
1.6 Toxicity and Environmental Impacts 13
1.7 Nanoparticles and Remediation of Azo-Dyes 14

CHAPTER 2

MATERIALS AND METHODS

2.1 Synthesis of Nanoparticles 17
2.2 Characterization of Synthesized Nanoparticles 17
2.2.1 Fourier Transform Infrared Spectroscopy (FTIR) 17
2.2.2 Scanning Electron Microscopy (SEM) 18
2.2.3 X-ray Diffraction (XRD) 18
2.3 Dyes 18
2.3.1 Preparation of Red, Yellow and Blue Dye Solutions 18
2.3.2 Preparation of Mix Dye Solutions 18
2.3.3 Preparation of Different pH Dye Solutions 18
2.4 Analysis of Dye Solutions Treatment by Nanoparticles 19
2.4.1 pH 19
2.4.2 Total Dissolved Solids (TDS) 19
2.4.3 Electrical Conductivity (EC) 19

2.4.4 Chemical Oxygen Demand (COD) 20
2.4.5 Decolourisation 20

CHAPTER 3

RESULTS AND DISCUSSIONS

3.1 Synthesized Nanoparticles 21
3.2 Characterization of Nanoparticles 21
3.2.1 Fourier Transform Infrared Spectroscopy (FTIR) 21
3.2.2 Scanning Electron Microscopy (SEM) 23
3.2.3 X-ray Diffraction (XRD) 25
3.3 Analysis of Dye Solutions Treatment by Nanoparticles 26
3.3.1 pH 26
3.3.2 Total Dissolved Solids (TDS) 28
3.3.3 Electrical Conductivity (EC) 29
3.3.4 Chemical Oxygen Demand (COD) 30
3.3.5 Decolourisation 30
3.4 Effect of pH on treatment 31
3.4.1 Effect of Acidic conditions 3pH and 5pH 31
3.4.1.1 Total Dissolved Solids of 3pH Dye Solutions 32
3.4.1.2 Electrical Conductivity of 3pH Dye Solutions 32
3.4.1.3 Chemical Oxygen Demand of 3pH Dye Solutions 33
3.4.1.4 Decolourisation of 3pH Dye Solutions 33
3.4.1.5 Total Dissolved Solids of 5pH Dye Solutions 34
3.4.1.6 Electrical Conductivity of 5pH Dye Solutions 35
3.4.1.7 Chemical Oxygen Demand of 5pH Dye Solutions 35
3.4.1.8 Decolourisation of 5pH Dye Solutions 36
3.4.2 Effect of Basic conditions 9pH and 11pH 36

3.4.2.1 Total Dissolved Solids of 9pH Dye Solutions 37

3.4.2.2 Electrical Conductivity of 9pH Dye Solutions 37

3.4.2.3 Chemical Oxygen Demand of 9pH Dye Solutions 38

3.4.2.4 Decolourisation of 9pH Dye Solutions 38

3.4.2.5 Total Dissolved Solids of 11pH Dye Solutions 39

3.4.2.6 Electrical Conductivity of 11pH Dye Solutions 40

3.4.2.7 Chemical Oxygen Demand of 11pH Dye Solutions 40

3.4.2.8 Decolourisation of 11pH Dye Solutions 41

CONCLUSION 44

RECOMMENDATIONS 45

REFERENCES 46

FIGURES

		Page
Figure 3.1.	Synthesized Iron Oxide Nanoparticles.	21
Figure 3.2.	FTIR spectrum of synthesized NPs.	22
Figure 3.3.	Scanning Electron Microscopy image A.	23
Figure 3.4.	Scanning Electron Microscopy image B.	24
Figure 3.5.	X–ray diffraction analysis of synthesized NPs.	25
Figure 3.6.	pH of different dye solutions before and after treatment.	27
Figure 3.7.	TDS of different dye solutions before and after treatment.	28
Figure 3.8.	EC of different dye solutions before and after treatment.	29
Figure 3.9.	COD of different dye solutions before and after treatment.	30
Figure 3.10.	UV absorbance of different dye solutions before and after treatment.	31
Figure 3.11.	TDS of different dye solutions of 3pH variable before and after treatment.	32
Figure 3.12.	EC of different dye solutions of 3pH variable before and after treatment.	32
Figure 3.13.	COD of different dye solutions of 3pH variable before and after treatment.	33
Figure 3.14.	UV absorbance of different dye solutions of 3pH variable before and after treatment.	34
Figure 3.15.	TDS of different dye solutions of 5pH variable before and after treatment.	34
Figure 3.16.	EC of different dye solutions of 5pH variable before and after treatment.	35
Figure 3.17.	COD of different dye solutions of 5pH variable before and after treatment.	35
Figure 3.18.	UV absorbance of different dye solutions of 5pH variable before and after treatment.	36
Figure 3.19.	TDS of different dye solutions of 9pH variable before and	37

after treatment.
Figure 3.20. EC of different dye solutions of 9pH variable before and after treatment. 37
Figure 3.21. COD of different dye solutions of 9pH variable before and after treatment. 38
Figure 3.22. UV absorbance of different dye solutions of 9pH variable before and after treatment. 39
Figure 3.23. TDS of different dye solutions of 11pH variable before and after treatment. 39
Figure 3.24. EC of different dye solutions of 11pH variable before and after treatment. 40
Figure 3.25. COD of different dye solutions of 11pH variable before and after treatment. 41
Figure 3.26. UV absorbance of different dye solutions of 11pH variable before and after treatment. 41

TABLES

		Page
Table 1.1.	Chemical Classification of Dyes.	10
Table 3.1.	Comparison of results before and after treatment of Dyes Solutions based on percentage.	42
Table 3.2.	Comparison of results before and after treatment of Dyes Solution of 3pH.	42
Table 3.3.	Comparison of results before and after treatment of Dyes Solution of 5pH.	42
Table 3.4.	Comparison of results before and after treatment of Dyes Solution of 9pH.	43
Table 3.5.	Comparison of results before and after treatment of Dyes Solution of 11pH.	43

CHAPTER 1

INTRODUCTION

The competitive environment of the planet is changing by fundamental technological, political, regulatory, and economic forces. The metamorphosis of economic landscape is not seen before. The scope of Industrial Revolution spans over two decades and this period is referred as a modern industrial revolution, and I predict it will take decades for these forces to be fully worked out in the worldwide economy (Jensen, 1993).

The modern world is facing a lot of problems and environmental pollution is one of the major and most urgent issues today. The greatest polluters are the industries, among which textile industries are the ones that are generating high liquid effluent pollutants due to the large quantities of water used in fabric processing. In the textile industry, wastewater with different composition is produced from different sections, from which coloured water released during the dyeing of fabrics may be the most problematic since even a trace of dye can remain highly visible. Other industries such as paper and pulp mills, dyestuff, distilleries, and tanneries are also producing highly coloured wastewaters. It is in the textile industry that the largest quantities of aqueous wastes and dye effluents are discharged from the dyeing process, with both strong persistent colour and a high biological oxygen demand (BOD), both of which are aesthetically and environmentally unacceptable (Hawks, Wang, Cochran, Harpending, & Moyzis, 2007). In general, the final textile waste effluent can be broadly categorized into 3 types, high, medium and low strength on the basis of their COD.

Industries are the major sources of pollution in all environments. Different industries discharge different types of pollutants directly or indirectly to the environment. Industrial waste includes employees' sanitary waste, process wastes from manufacturing, wash waters and relatively uncontaminated water from heating and cooling operations.

The industry that has the most complicated manufacturing process is the textile industry because of its fragmented and heterogeneous character. The wet process of textile finishing industry causes major impacts on environment. The waste from the

textile processing is directly discharged to a nearby water body or indirectly to municipal sewage treatment plant (Ahmad & Puasa, 2007).

The major effluents discharged from the textile industries comprise of colour dyes. The potential impacts of these dyes are usually carcinogenic. Some of these dyes can undergo anaerobic decolourization that result in the formation of carcinogens. These coloured dyes can block sunlight penetration and oxygen dissolution in the water that are important for the aquatic life (Abdulraheem, Peter Obinna, Kasali Ademola, & Kasali Ademola, 2012).

Various synthetic dyes are extensively used in textile dyeing, paper, pulp, plastic, colour photography, pharmaceutical, food, cosmetic and other industries. It is reported that there are over 100,000 kinds of commercial dyes with a rough estimated production of 7 × 105–1 × 106 tons worldwide annually. Although azo dyes represent approximately 60–70% of all dyes used by the textile industry, anthraquinone dyes are becoming more and more important because of their bright colour, high fixation rate and strong colour fastness. Following after azo and anthraquinone dyes, triphenylmethane dyes are classed as the third dyes as far as dye consumption is concerned (He et al., 2012).

Even a very low concentration of these dyes in water is undesirable. Over 70,000 tons of approximately 10,000 types of dyes and pigments are produced annually worldwide. During the process of curing and finishing in the industry, about 20 - 30% of these dyes are discharged in industrial effluents as waste (Manohar and Shrivastava. 2015).

Under typical manufacturing and dyeing process, there are estimated 10–20% of the dyes entering the environment through wastewater, resulting in large amounts of dye-containing wastewater. Considering the increasingly strict legislations and regulations, the associated industries are required to find economically viable wastewater treatment methods to solve SS, COD and aesthetic problem. However, most dyes are known for their stability to light, heat and difficulty to biodegrade. Also, dyes' breakdown products may be toxic and even carcinogenic to aquatic life. Therefore, effective and efficient decolourization processes for azo, anthraquinone and triphenylmethane dyes need to be developed (He et al., 2012).

Change in water colour due to these dyes is one of the most obvious physical indicators of water pollution. The discharge of these dyes causes damage to the receiving water bodies and the aquatic life living there. Dye-water pollution is becoming alarming due to increased use of these colour dyes. Other than textile industries another major source of release of these dyes is dyestuff manufacturing industries. These dyes are difficult to treat through microbial degradation due to presence of substitutions such as azo, nitro or sulphur group (Nigam, Banat, Singh, & Marchant, 1996).

The textile industries use azo dyes that are organic in nature and are considered as carcinogenic substances. The azo-linkage on reduction releases aromatic amines that causes liver cancer in human (Dinesh, Anandan, & Sivasankar, 2015).

These azo dyes are restricted in European countries due to the derivative compounds of this substance, such as aromatic amine and phenol. These are mutagens and carcinogens and enter the food web via aquatic life living in the affected water bodies and are a risk to humans due to substances of very high concern. In Thai the government has forced the textile industries to treat the effluent before releasing it into the public water system as per required standards (Department of Industrial Works 2007).

The by-products that are released on degradation of azo dyes have dangerous impacts on humans as well as on environment. The aromatic amines are the main substitutes that cause the problem. The removal rate of these materials during aerobic treatment is still very low (Dalali, Khoramnezhad, Habibizadeh, & Faraji, 2011).

These effluents must be treated before they are released into the surrounding environment. Different techniques and approaches have been used to decontaminate effluents from the textile industries. Adsorption, coagulation, ion flotation, sedimentation, co-precipitation, electrochemical treatment, Sono-chemical treatment and photo catalytic area few among a number of techniques that are used for treatment of these pollutants (Premkumar, Rajan, & Ramesh, 2016).

1.1 Nanoparticles

Due to the novel mesoscopic properties of magnetic nanoparticles, its synthesis has been a field of intense study. Nano-sized particles have physical and chemical

properties that are characteristic of neither the atom nor the bulk counterparts (Kim, Zhang, Voit, Rao, & Muhammed, 2001).

Based on their unique mesoscopic physical, tri-biological, thermal, and mechanical properties, super paramagnetic nanoparticles offer a high potential for several applications in different areas such as Ferro-fluids, colour imaging, magnetic refrigeration, detoxification of biological fluids, magnetically controlled transport of anti-cancer drugs, magnetic resonance imaging contrast enhancement and magnetic cell separation (Laurent et al., 2008).

Nanoparticles are becoming key components in a wide range of applications. Research encompasses numerous disciplines, e.g. nanotechnology, molecular engineering, medicine, pharmaceutical drug manufacture, biology, chemistry, physics, optical components, polymer science, mechanical engineering, toxicology, cosmetics, energy, food technology and environmental and health sciences (IJNP).

Nanotechnology is the science that deals with matter at the scale of 1 billionth of a meter (i.e., $10 - 9$ m = 1 nm), and is also the study of manipulating matter at the atomic and molecular scale. In general, the size of a nanoparticle spans the range between 1 and 100 nm. Metallic nanoparticles have different physical and chemical properties from bulk metals (e.g., lower melting points, higher specific surface areas, specific optical properties, mechanical strengths, and specific magnetizations), properties that might prove attractive in various industrial applications (Satoshi Horikoshi and Nick Serpone).

1.1.1 Iron Oxide Nanoparticles

Nanomaterials may be significantly more reactive than larger particles because of their much greater surface area per unit of mass (Ricker by and Morrison 2007).

Iron oxides are common compounds, which are widespread in nature and can be readily synthesized in the laboratory. Particularly, bio applications based on magnetic nanoparticles (NPs) have received considerable attention because NPs offer unique advantages over other materials. For example, magnetic IONPs are inexpensive to produce, physically and chemically stable, biocompatible, and environmentally safe. Iron oxides are known, among these iron oxides Fe_3O_4 and Fe_2O_3) are very promising and

popular candidates due to their polymorphism involving temperature-induced phase transition.

1.1.2 Characterization of Iron Oxide Nanoparticles

UV-Vis spectrometry is used in analytical chemistry to characterize materials. In Ultraviolet-Visible Light Spectroscopy, either one or two light sources are used to emit light over the ultraviolet and visible light spectra (200-800nm).

$$Absorbanc = -log10\ (I\ /Io) = Concentration \cdot \varepsilon \cdot l$$

The incident light (Io) is the maximum intensity of light that passes through sample and is absorbed by the sample. The concentration on analyte within the sample is solved with the help of beer-lambert law, equation 1, and the intensity of transmitted light is used. The path length which is the distance travelled by the light through the cuvette that is mostly 1cm, is required for the relationship. The molar extinction coefficient (ε) of the analyte, which is a measurement of how strongly the analyte absorbs light at the specific wavelength, is also required. Solutions of transition metal and organic compounds are also characterized with the help UV-Vis Spectroscopy. Solutions of transition metals tend to have distinct colour characteristics and therefore corresponding peaks. Organic compounds are differentiated by their bond structures and functional groups when analysing the peaks in a given spectrum (Modern Chemical Techniques, 1998).

1.1.2.1 Optical Properties of Iron Oxide Nanoparticles

The optical property of the Fe_2O_3 nanoparticles is one of the important characteristics for the evaluation of its optical and photocatalytic activity. UV/visible absorption are a method in which the outer electrons of atoms or molecules absorb radiant energy and undergo transitions to high energy levels. In this procedure, the spectrum obtained owing to optical absorption can be analysed to acquire the energy band gap of the semiconductor nanomaterial. The optical absorption measurement was carried out at room conditions. Therefore, the nanomaterial may be helpful for the development of non-linear optical sensors in this wavelength region, as the lack of

absorption peaks is the major prerequisite for the nanomaterial to confirm non-linear properties (Mohammed M. Rahman et al.).

Mohammed M. Rahman et al. also reported that it displays an onset of absorption maxima at 404.0 nm in visible range between 200 to 800 nm wavelengths. The lambda maxima of as grown NPs are quite different to those observed earlier due to Fe_2O_3 and Fe_3O_4 (Cherepy et al., 1998) but are very similar to those reported for Fe_2O_3 (Cornell & Schwertmann, 2003). It shows a broad absorption band around 404.0 nm indicating the formation of low dimensional Fe_2O_3 NPs having reddish colours. Band gap energy is calculated on the basis of the maximum absorption band (404nm) of Fe_2O_3 NPs and obtained to be 3.06931 eV, according to following equation.

$$Ebg = 1240/E \text{ . (eV)}$$

Where Ebg is the band-gap energy and λmax is the wavelength (404.0 nm) of the nanoparticles.

K.Tharani, L.C. Nehru reported that optical properties of Fe_2O_3 sample were determined through UV-VIS. The optical absorption spectra were recorded by using shimadzu-pharmaspec-17000 UV-VIS.

Optical absorption coefficient has been calculated in the wavelength region 200-900nm. The band gap of the nanoparticles as prepared are determined from the relation.

$$(\alpha h\gamma)2 = C(h\gamma - Eg)$$

Where, C is a constant, Eg is the band gap of the material. α is the absorption co-efficient. At 272nm in the UV-vis spectrum presence of maximum absorption is observed.

1.1.3 Synthesis of Iron Oxide Nanoparticles

1.1.3.1 Iron Oxide Nanoparticles-Thermal Decomposition Method

The UV-Vis spectrum tells us the absorbance pattern of the iron oxide nanoparticles synthesized using the thermal decomposition method. The spectrum is

obtained by the process that involves a 1:11 dilution of iron solution, from the centrifugation process, into hexane.

1.1.3.2 Iron Oxide Nanoparticles-Co-Precipitation Method

The absorbance pattern of the iron oxide nanoparticles synthesized utilizing the co-precipitation method can be observed on spectrum. The dilutions of this sample differed for it was a very dark concentrated black at the end of the synthesis process. The dilution of the sample followed as 50 μL in 2 mL of water (1:40) followed by an additional dilution of 1:4 using the previous dilution and water respectively. This allowed for the desired absorbance peak at around 0.5 seen below.

1.2 Dyes

A dye is a coloured substance that has an affinity to the substrate to which it is being applied. The dye is generally applied in an aqueous solution, and may require a mordant to improve the fastness of the dye on the fibre (Booth, Zollinger, McLaren, Sharples, & Westwell, 2000a).

1.2.1 History of Dyes

In 1834 RUNGE isolated aniline from coal tar and observed the formation of aniline black on oxidation. Picric acid was used as a silk dye in 1849. The first synthetic dye of technical significance, called Mauveine after its mauve colour, was obtained in 1856 by PERKIN in an attempt to synthesize quinine. With his father and brother, he founded the first factory to manufacture synthetic dyes in Greenford Green, near London.

This was the start of the dye and pigment industry. The year 1856 also saw the synthesis of fuchsine. The manufacture of fuchsine, later called magenta, began in 1859. In 1862 GRIESS created azo dye chemistry with the discovery of diazo compounds.

Among the earliest azine dyes were induline in 1863 and nigrosine in 1867. The first synthesis of an anthraquinone dye was that of alizarin in 1868. The first sulphur dye was obtained in 1873, and indigo was synthesized in 1878. Progress became very rapid with the advent of structural organic chemistry; many thousands of dyes were synthesized within a few decades. Many of the large chemical plants in operation in Germany and

Switzerland today were built as dye factories in the second half of the 19th century. The manufacture of dyes has spread from Europe throughout the world; Western Europe still accounts for ca. 40 % of the worldwide total (Booth, Zollinger, McLaren, Sharples, & Westwell, 2000b).

Wastewater from the textile industry is a complex mixture of many polluting substances ranging from organochlorine-based pesticides to heavy metals associated with dyes or dying process (Correia, Stephenson, & Judd, 1994).

1.2.2 Usage in Textile

Industrialization of the textile industry and use of a large variety of chemical treatments and dyes has resulted in a public health threat created by pollution. 17 -20% of industrial freshwater pollution is caused by textile dyeing and treatment. Estimations state that 10-15% of total dyestuffs (equivalent to 280,000 tons of dyestuffs) used during the manufacturing of textile products is released into the environment worldwide annually (Badruddoza, Tay, Tan, Hidajat, & Uddin, 2011),

The textile industry ranks first in the usage of dyes for coloration of the fibres. The textile sector alone consumes about 60% of total dye production for coloration of various fabrics and out of it, it is estimated that around 10–15% of dyes are wasted into the environment upon completion of their use in the dyeing unit which generates a strongly coloured wastewater, typically with a concentration in the range of 10–200 ppm or mg/L (Amit Kumar Dutta).

1.2.3 Types

Dyes are complex unsaturated aromatic compounds fulfilling characteristics like intense colour, solubility, substantiveness and fastness. Dyes can be defined as the different type of colouring particles which differ in each type from the other in chemical composition and are used for colouring fabrics in different colours and shades which are completely soluble in liquid media. Dyes can be classified into (Kirk-Othmer, 1979).

1.2.3.1 Acid Dyes

Anionic dyes, soluble in water, with one or more sulphonic or carboxylic acid groups in their molecules and, chemically, constituted by compounds azo, anthraquinones and triarylmethanes, iminoacetone, nitro, nitrous and quinoline, with application in nylon, silk, modified acrylic, wool, paper, food and cosmetics.

1.2.3.2 Basic Dyes

Cationic dyes, soluble in water, producers of colouring cationic compounds in solution and chemically constituted by compounds azo, anthraquinone, triarylmethane, methane, thiazine, oxazine, acridine and quinoline, with application in modified acrylic, modified nylon, modified polyesters and papers, and some of them having biological activity are used in medicine as antiseptics.

1.2.3.3 Direct Dyes

Anionic compounds, soluble in water, when in the presence of electrolytes increase the affinity for the fibre. Chemically are constituted by azo compounds, with thiazoles, phtalocyanines and oxazines, with application in the dyeing of cotton and regenerated cellulose, paper, leather and nylon.

1.2.3.4 Fluorescent Dyes

Colourless compounds (belongs from Xanthenes group) that absorb incident ultraviolet light and re-emit in the visible region (blue) of the spectrum. In fact, they are not dyes, but due to the wide application in fabrics and other materials, the Colour Index made their classification within this group of chemicals.

1.2.3.5 Reactive Dyes

Compounds with very simple chemical structure and absorption spectrum presents narrow range of capitation and dyeing possessing brilliant characteristics. Chemically are constituted by azo compounds, anthraquinones and phtalocyanines, with high fixing property by simple dyeing methods, making covalent bridges with the fibre (cotton, wool or nylon), by the compatible hydroxyl group of cellulose.

1.2.3.6 Sulphurous Dyes

Small group of dyes, however, with low cost and good fixing properties can be applied to cotton, after alkaline reduction bath, with sodium sulphite as reducing agent.

1.2.3.7 Vat Dyes

Insoluble compounds in water and applied, mainly, to cellulosic fibres, such as leuco-soluble salts, after reduction in alkaline bath, normally with sodium hydrosulphite. After exhaustion of the fibre, they are re-oxidized to the keto-insoluble form and after treatment normally by soda, develop crystalline structure. Chemically are the anthraquinones and indigo.

1.2.3.8 Dye Precursors

Dyes obtained from raw materials. This group has simple chemical characteristic, such as benzene and naphthalene, whose colour is given by a variety of chemical reactions. Normally they are cyclic aromatic compounds and derivatives, mainly of petroleum and coal.

1.2.3.9 Further Chemical Classification

Table 1.1. Chemical Classification of Dyes.

Sources	**Types**
Textiles and Leather Industry	Anthraquinone dyes, Arylmethane dyes, Azo dyes , Acridine dyes, Cyanine dyes, Diazonium dyes, Nitro dyes, Nitroso dyes
Paper Industry	Phthalocyanine dyes, Quinone-imine dyes
Cotton, Silk and Wool Industry	Xanthene dyes
Color Photography	Indophenol dyes, Oxazone dyes
Printing Press Industry	Oxazin dyes, Thiazin dyes
Others	Thiazole dyes, Fluorene dyes, Rhodamine dyes, Pyronin dyes

1.3 Remediation

A wide range of technologies has been developed for the removal of synthetic Azo-Dyes from waters and wastewaters to decrease their environmental impact (Pereira & Alves, 2012).

1.3.1 Physical Methods

Such as membrane-filtration processes (Nano-filtration, reverse osmosis, electro dialysis) and sorption techniques.

1.3.2 Chemical Methods

Such as coagulation or flocculation combined with flotation and filtration, precipitation-flocculation with $Fe(II)/Ca(OH)_2$, electro-flotation, electro-kinetic coagulation, conventional oxidation methods (e.g. with ozone), irradiation or electrochemical processes.

1.3.3 Biological Methods

Aerobic and anaerobic microbial degradation and use of pure enzymes.

1.4 Remediation of Organic Compounds

Maintaining and restoring the quality of air, water and soil is one of the great challenges of our time. Most countries face serious environmental problems, such as the availability of drinking water, the treatment of waste and wastewater, air pollution and the contamination of soil and groundwater. In many cases, conventional remediation and treatment technologies have shown only limited effectiveness in reducing the levels of pollutants, especially in soil and water. Nanotechnology promises a potential revolution in approaches to remediation (Nicole C. Mueller* and Bernd Nowack).

Nanomaterials unique properties allow them to remove pollutants from the environment. Silver, iron, gold, titanium oxides and iron oxides are some of the commonly used Nano scale metals and metal oxides cited by the researchers that can be used in environmental remediation. The researchers suggest that nanoparticles can be attached to host polymer materials, such as porous resins, cellulose and silica, to reduce

potential harm to human health and the environment derived from the release of nanoparticles into the environment.

Silver nanoparticles, for example, have proved to be effective antimicrobial agents and can treat wastewater containing bacteria, viruses and fungi. Nanoscale titanium dioxide can also kill bacteria and disinfect water when activated by light. Gold nanoparticles may potentially be another useful material for removing contaminants, such as toxic chlorinated organic compounds, pesticides and inorganic mercury, from water. They can also be used to remediate air. In combination with titanium dioxide, gold nanoparticles have been shown to convert the toxic air pollutant, sulphur dioxide, to sulphur. Titanium dioxide nanomaterials are commonly used in some processes to disinfect water, in addition to breaking down halogenated compounds, and removing dyes and metal toxins from drinking water and wastewater (Khin, Nair, Babu, Murugan, & Ramakrishna, 2012).

The nanoparticles fixed to the host material are thus bulkier and can be more easily removed and captured from wastewater. Nanoparticles, such as Nano scale zinc oxide, fixed in this way, are used, for example, to break down organochlorine pesticides, halogenated herbicides and azo dyes. In addition to remediating pollution, nanoparticles can be used as sensors to monitor toxins, heavy metals and organic contaminants in land, air and water environments and have been found to be more sensitive and selective than conventional sensors. Sensor strips composed of nylon 6 Nano-fibre nets are one example.

These are used to detect formaldehyde, a toxic air pollutant widely used in the manufacture of household materials and building products. The yellow sensor strips turn red upon exposure to formaldehyde (Khin et al., 2012).

1.5 Azo-Dyes

Azo dyes are compounds characterized with the presence of one or more azo groups (-N=N-), usually in number of one or four, linked to phenyl and naphthyl radicals, which are usually replaced with some combinations of functional groups including: amino (-NH2), chlorine (-Cl), hydroxyl (-OH), methyl (-CH3), nitro (-NO2), sulphonic

acid and sodium salts (- SO3Na) (G. M. Shaul 1986). Azo dyes, synthesized from aromatic compounds, are not basic in aqueous solution (due to the presence of the linkage N=N, which reduces the possibility of unpaired electron pairs in nitrogen atoms), are readily reduced to hydrazines and primary amines, functioning as good oxidizing agents (USEPA. 2008).

1.6 Toxicity and Environmental Impacts

Colour in the effluent is one of the most noticeable indicators of water pollution and the discharge of highly coloured synthetic dye effluents is aesthetically very unpleasing and can damages the receiving water body by hindering the penetration of light. Moreover, dyes are stable, recalcitrant, colorant, and even potentially carcinogenic and toxic. Their release into the environment creates serious environmental, aesthetical and health problems. Thus, industrial dye-laden effluents are an increasingly major concern and need to be effectively treated before being discharged into the environment in order to prevent these potential hazards (A. Buekens).

The potential accumulation of azo dyes in the environment was viewed with concern and resulted in research sponsored by the American Dye Manufacturers Institute (ADMI) and the Ecological and Toxicological Association of the Dyestuffs Manufacturing Industry (ETAD). Several studies supported by ADMI suggested that the toxicity of commercial dyes to fish and mammals was minimal. They concluded that commercial dyes, with the exception of benzidine dyes and the triphenylmethane type of cationic dyes, were not generally hazardous chemicals. One of the triphenylmethane dyes was found to be toxic to freshwater fish.

Benzidine and some of its derivatives were found to be mammalian carcinogens. Azo reduction of a large number of azo dyes results in the formation of benzidine and benzidine derivatives [25]. As a further caution, it should be noted that toxicity data at chronic low-level exposures for most of the commercial dyes and their derivatives are lacking. Dyes in aquatic environments were reported to affect microbial populations and their activities. Azo dyes such as Basic Brown 4 (C.I. 21010), Direct Brown 95 (C.I. 30145), Direct Black 80 (C.I. 31600), Mordant Black 11 (C.I. 14645), Acid Black 52 (C.I. 1571 l), Direct Red 81 (C.1. 28160), and Direct Yellow 106 were inhibitory to

microbial oxidation processes in both activated sludge and stream water (Chung & Stevens, 1993).

Studies showed the presence of some azo dyes in certain algae and plants (P.N. Srivastava, 1991) and also have shown the adverse effects for aquatic microbial populations exposed to effluents containing dyes (G.B. Michaels and D.L. Lewis, 1985). Several studies show that the release of azo dyes into the environment is alarming due to the toxic, mutagenic and carcinogenic characteristics of these dyes and of their biotransformation products (Y.H. Lin and J.Y. Leu, 2008), which can cause different damages to the organisms exposed.

Oral exposure of humans to azo dyes can lead to the formation of aromatic amines, both by the intestinal microflora and by liver azoreductases and some of these amines have presented carcinogenic properties (J.K. Lin and Y.H. Wu, 1973).

Several azo dyes present genotoxic, mutagenic and carcinogenic activity in tests with microorganisms and mammalian cells (S. Venturini and M. Tamaro, 1979). The 3-methoxy-4- amino-benzene, for example, is mutagenic for bacteria and carcinogenic for rats, while 2-methoxy-4- amino-benzene is weakly mutagenic for bacteria but not carcinogenic for rats (Y. Hashimoto, 1977). Thus, the genotoxicity, mutagenicity and carcinogenicity of dyes are closely related with the nature and position of the substituent bond to the azo group (G.A. Umbuzeiro, 2005).

The majority of dyes pose a potential health hazard to all forms of life (Prakash, 1993). These dyes may cause allergic responses, skin dermatoses, eczema (Su and Horton, 1998), and may affect the liver, the lungs, the vasco-circulatory system, the immune system and the reproductive system of experimental animals as well as humans (Nikulina et al., 1995).

1.7 Nanoparticles and Remediation of Azo-Dyes

The precipitation method was adopted for synthesis of iron oxide nanoparticles. Synthesized iron oxide nanoparticles were characterized by using Scanning Electron Microscopy (SEM), Energy Dispersive X-Ray Spectroscopy (EDX) and Fourier Transform Infrared Spectroscopy (FTIR). The physio–chemical parameters were

determined using standard methods. Role of iron oxide nanoparticles (Dosage- 250&500 mg) on physio-chemical parameters of textile Dyeing Industry effluent. The role of different dose (250&500mg) of iron oxide nanoparticles on the physio-chemical parameters of Textile Dyeing Industry effluent such as colour, pH, electrical conductivity, COD and calcium were estimated after exposing the effluent in the sunlight for a period of half an hour.

The colour of the effluent is reddish brown, light brown and no colour for control, low and high dose iron oxide nanoparticles respectively. The pH in control is 7.3 and the pH decreased with increasing dose of iron nanoparticles. The electrical conductivity is 2900, 2200 and 1600 in control, low and high dose respectively. Like electrical conductivity the COD and Calcium content in the effluent decreased with increasing dose of textile dyeing industry effluent.

The result indicated that iron oxide nanoparticles was effective to reduce the colour, pH, electrical conductivity, COD and calcium chemically synthesized iron nanoparticles can be used for the removal of contaminants present in the textile dyeing industry effluent. Kale et al (2014) reported the decolourization of dye using nickel nanoparticles.

Fan et al (2009) also reported the rapid decolourization of azo dye methyl orange in aqueous solution by nanoscale zero valent iron particles. From the present study, the physio-chemical parameters were reduced with increasing dose of iron oxide nanoparticles (M.R. Rajan et al.).

Objectives of Study

1. To synthesis iron oxide nanoparticles for the treatment of azo reactive dyes.
2. Characterization of synthesized iron oxide nanoparticles.
3. To evaluate the potential of iron oxide nanoparticles in de-coloration of azo reactive dyes.
4. To evaluate the effect of pH on de-coloration potential of iron oxide nanoparticles.

CHAPTER 2

MATERIAL AND METHODS

2.1 Synthesis of Nanoparticles

Iron oxide nanoparticles were synthesized by co-precipitation method in the laboratory. 12gms of ferric chloride ($FeCl_3$) was dissolved in 150ml of distilled water and the solution was vigorously stirred using magnetic stirrer for 20mins to attain the pH of 3. Precipitation of iron oxide nanoparticles was achieved by adding 100ml solution of 2M sodium hydroxide solution drop wise under vigorously stirring. The final pH of the solution was maintained at 12 to achieve maximum precipitation. The solution was kept on magnetic stirrer until the colour changed to dark brown indicating formation of iron oxide nanoparticles.

The prepared nanoparticles were recovered by centrifuging the solution at 1500 rpm for 20min. The supernatant was discarded and the pellet was obtained and dried on a clean dry plastic sheet. The particles were oven dried at 70°C for 30 minutes. The dried iron oxide nanoparticles were grinded in mortar and pestle to obtain a homogeneous size before characterisation. The characterization of nanoparticles was done to analyse their characteristics.

2.2 Characterization of Synthesized Nanoparticles

Synthesized nanoparticles were characterised using Fourier Transform Infrared Spectroscopy (FTIR), Scanning Electron Microscopy (SEM) and X-rays diffraction (XRD) methods. These three methods were performed under strict supervision in order to reduce chances of error. The results were interpreted to observe the characteristics of nanoparticles.

2.2.1 Fourier Transform Infrared Spectroscopy (FTIR)

The FTIR method was used to detect chemical composition of nanoparticles. This analysis was done in an FTIR Perkin Elmer Spectrum 100 spectrometer. The peak variations of NPs at distinct pH values were examined.

2.2.2 Scanning Electron Microscopy (SEM)

The morphology and composition of Iron Oxide nanoparticles were examined by Scanning Electron Microscopy (SEM). This was performed using Jeol Jed 2300 in the laboratory and the results were interpreted.

2.2.3 X-ray Diffraction (XRD)

XRD was performed using X'pert PRO PANalytical to obtain the crystalline structure of the particles. In a diffraction pattern, the intensity can be used to quantify the proportion of iron oxide formed in a mixture by comparing experimental peak and reference peak intensities.

2.3 Dyes

2.3.1 Preparation of Red, Yellow and Blue Dye Solutions

The two different dyes solutions were prepared in the laboratory with different concentrations. Tap water was used for the preparation of dyes solutions. All the dyes solutions were prepared in 100ml tap water with 5% and 10% dyes to differ the concentration. Pipette was used to measure 5ml of each red, yellow and blue dye. Total 6 solutions were made, first three with 5% concentration and other three with 10% concentration.

2.3.2 Preparation of Mix Dye Solution

The mix dye solution was prepared by adding 5% of each colour that is red, blue and yellow dye in 100ml of tap water.

2.3.3 Preparation of Different pH Dye Solutions

Each dye solution was adjusted to different pH 3, 5, 9 and 11. Concentrated HCl acid was used to lower the pH and obtain the 3 and 5 pH. Where Concentrated NaOH was used to increase the pH at 9 and 11. The acid and Base were added to the solution drop wise, with the help of a dropper. Concentrated dyes solutions were prepared by adding 5% dye in 20ml of tap water to clearly observe the change. Dyes that were prepared were red, yellow, blue and mix. The mix dye solution was prepared by adding

5% red dye, 5% yellow dye and 5% blue dye in 20ml solution. With each colour dye including the mix dye solution 4 samples were prepared with different pH 3, 5, 9, and 11. A total of 16 solutions were prepared in different pH.

2.4 Analysis of Dye Solutions Treated by Nanoparticles

100mg of prepared nanoparticles were weighed using laboratory balance on a paper. The weight of paper was zeroed before the beginning using the zero buttons on balance. The weighed 100mg of nanoparticles were added to dye solutions. The dye solutions were kept on magnetic stirrer for 30 minutes with the stirrer on. pH, TDS, UV, COD and EC of the solutions were documented before and after the treatment.

2.4.1 pH

pH /TDS/EC meter was used to measure the pH of samples before and after the treatment to observe the change. The pH rod was first washed with distilled water to remove any impurities and to obtain more accurate results. The pH rod after washing was dipped into the sample solution one by one and readings were noted. The rod was washed every time for the next sample.

2.4.2 Total Dissolved Solid (TDS)

The total dissolved solids (TDS) were measured using TDS meter. The rod was washed with distilled water and then dipped into the sample solution. Readings were noted for each sample. For every sample TDS was noted before and after the treatment so that the change could be observed.

2.4.3 Electrical Conductivity (EC)

Electrical conductivity was also carried out using pH/TDS/EC meter. The rod was dipped into the sample solution after washing it properly with distilled water and readings were recorded. This experiment was performed with all the samples before and after treatment in order to observe the change.

2.4.4 Chemical Oxygen Demand (COD)

COD of water samples was determined by using digestion method, before and after the treatment. A sample of about 2.5ml was taken in a COD bottle, to which 2.5 ml strong digestion solution and 3.5 ml 0.1N H_2SO_4 COD solution was added. Then the COD bottle was kept in thermo reactor for 2 hrs. at 150°C for complete digestion. After that the solution was allowed to cool down and then COD was measured in mg/L through "spectroquantpharo 300".

2.4.5 Decolourisation

UV absorbance experimentation was conducted in Bahria University laboratory using UV4000 spectrophotometer. The experiment was performed by using wavelength of 480nm. The cell that was used was of glass. First the UV spectrophotometer was calibrated using distilled water in the cell. 2.5ml of sample solution was used in cell to obtain UV analysis. The sample was added in cell carefully to avoid any bubbles and was then dried using tissue papers.

CHAPTER 3

RESULTS AND DISCUSSIONS

3.1 Synthesized Nanoparticles

Figure 3.1. Synthesized Iron Oxide Nanoparticles.

The synthesized iron oxide nanoparticles were of dark brown colour and of homogeneous size. After the synthesis, characterization of iron oxide nanoparticles was performed to understand its morphology.

3.2 Characterization of Nanoparticles

3.2.1 Fourier Transform Infrared Spectroscopy (FTIR)

The infrared spectra of nanoparticles before the decolourisation process were observed in the range of 4000-450 cm^{-1}. The iron oxide nanoparticles show the vibrations at 3443.76 cm^{-1} and 1630.38 cm^{-1}.

The findings suggest that the vibration stretch at 3443.76 cm^{-1} it belongs to the function group of Alcohol, Phenol O-H and Amine N-H. The vibration stretch at 1630.38

cm^{-1} suggest that it belongs to the function group of Amide C=O, Aromatic C=C and Alkenyl C=C.

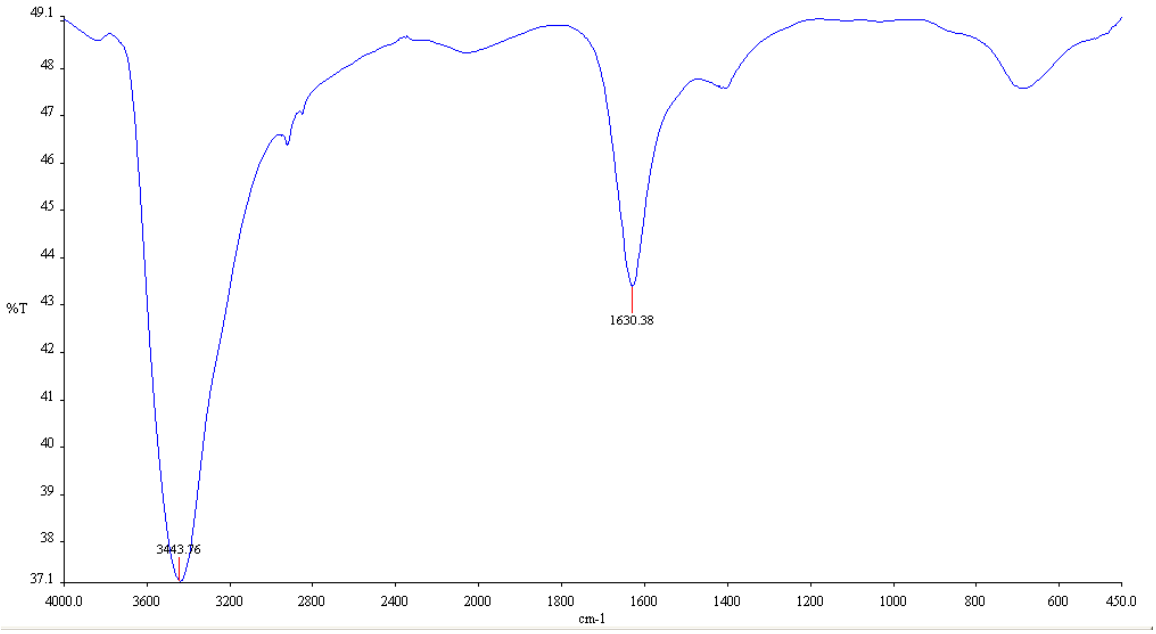

Figure 3.2. FTIR spectrum of synthesized NPs.

Study conducted by T. Shahwan et al., 2011 suggested that FTIR of GT-Fe NPs revealed several peaks in the spectral range 800-1800cm^{-1}. A strong peak at 1065cm^{-1} relates to the stretching vibration of C-O-C and that at 1220cm^{-1} is ascribed to the asymmetric stretching bands. At 1400cm^{-1} relates it to –OH in phenols and at 1600cm^{-1} can be attributed to C=C ring stretching in polyphenols.

The spectra obtained for GT-Fe NPs after contact with methylene blue solution showed spectral feature at 2925cm^{-1} and 2818cm^{-1}. These bands relate to the stretching vibration of C-H in the methyl groups (T. Shahwan et al., 2011).

The spectra obtained for GT-Fe NPs after contact with methyl orange solution showed spectral feature at 2927cm^{-1} that relates to asymmetric $–CH_3$ vibrations. In addition other peaks were observed at 697cm^{-1}, 629cm^{-1} and 572cm^{-1} that are attributed to –C-S- stretching vibrations (T. Shahwan et al., 2011).

FT-IR spectrum of magnetite nanoparticle shows that the characteristics peaks at 580cm^{-1} relate to Fe-O stretching vibration. The bands near 3395cm^{-1} and 1620cm^{-1} refer to the O-H stretching vibration (Bedabrata Saha et al., 2010).

The IR spectrum of Iron Oxide nanoparticles manifests prominent absorption band located at 3789, 3365, 30005, 1710, 1422, 1361, 1223, 1092, 862, 552 and 471cm-1. The strong band at 552cm-1 may resulted from (O-H) stretching vibration (K.Tharani, L.C. Nehru, 2015).

3.2.2 Scanning Electron Microscopy (SEM)

Analysis of the SEM image of synthesized iron oxide Nanoparticles showed a clear image of the nanoparticles range from 20nm to 80nm. The percentage beyond 80nm was very less. The image confirms that synthesized nanoparticles have the average size of 50nm.

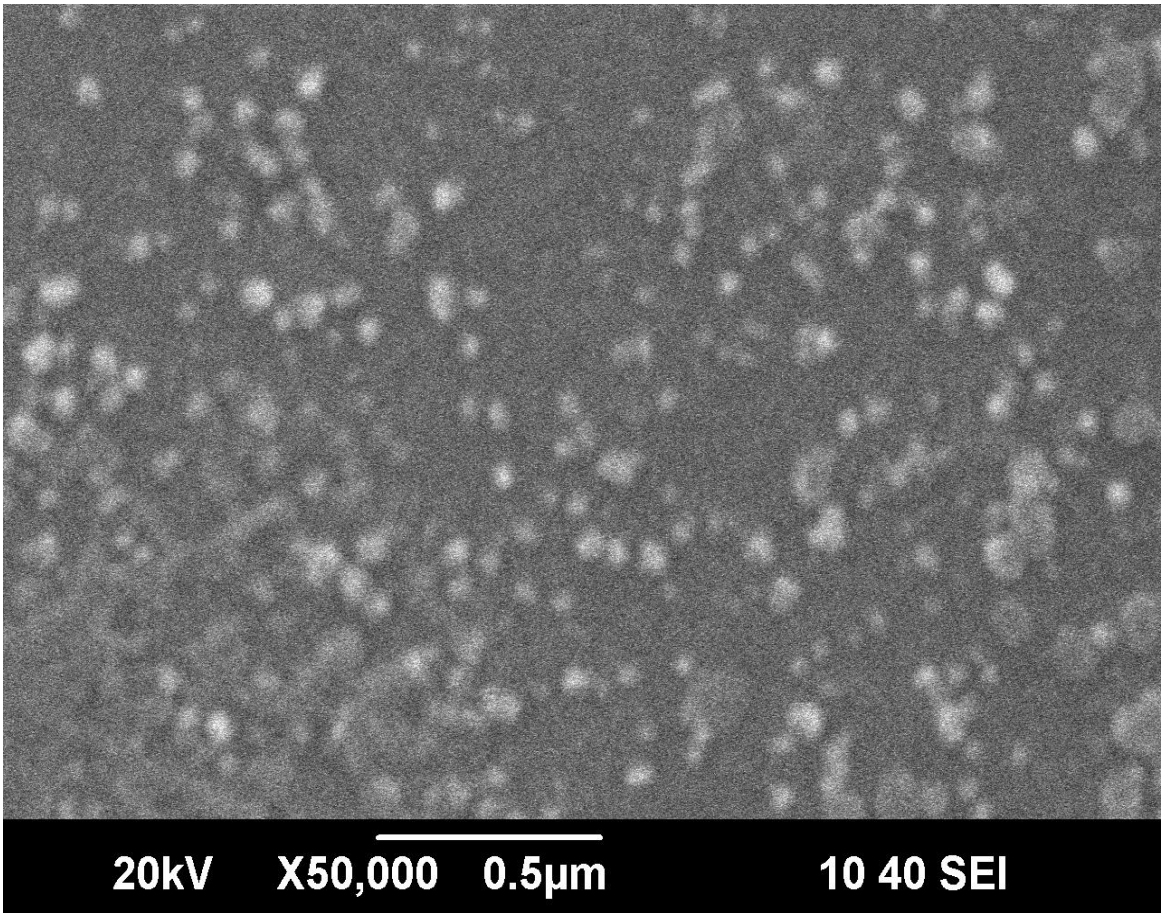

Figure 3.3. Scanning Electron Microscopy image A.

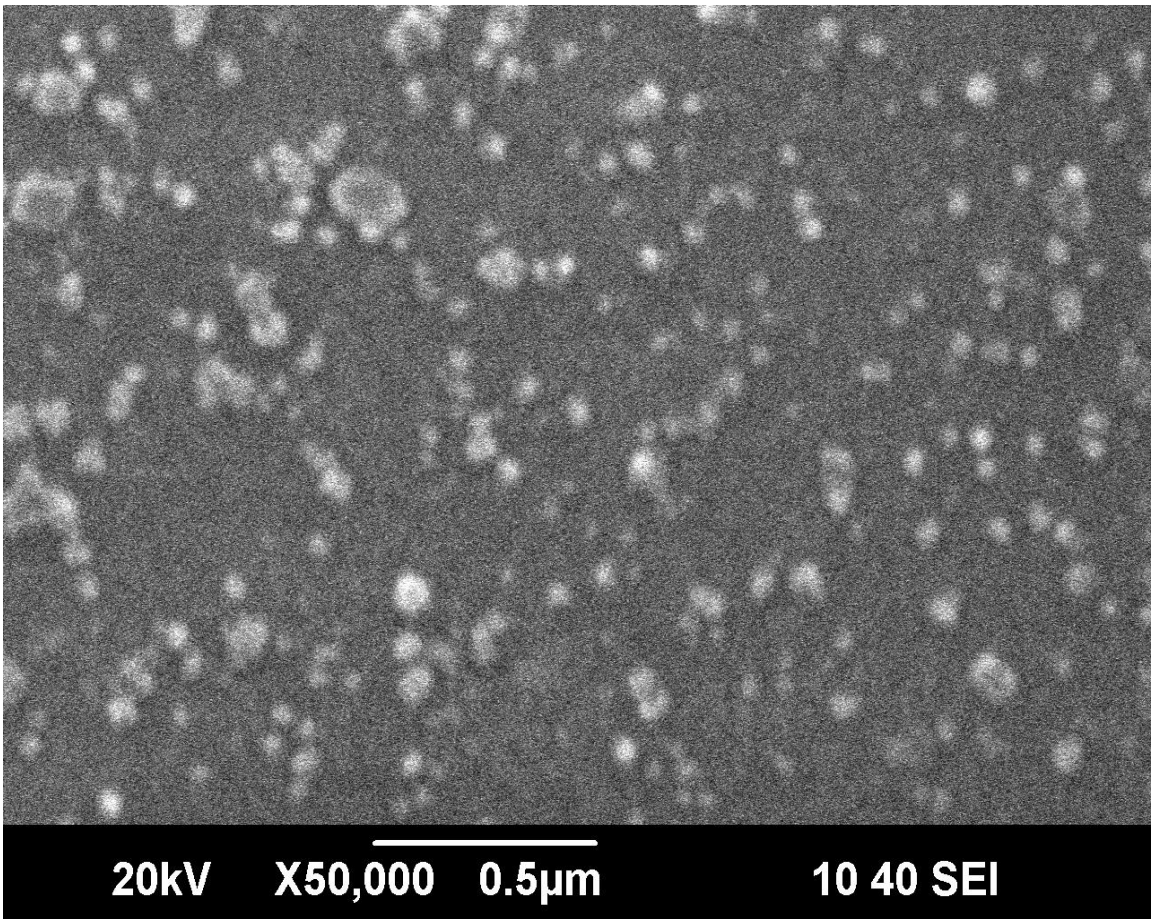

Figure 3.4. Scanning Electron Microscopy image B.

The reaction between ferrous chloride occurs within a few minutes at room temperature by increasing the pH and indicated by colour changes from brown to black colour. The high density of iron oxide nanoparticles was assumed by SEM. Obtained nanoparticles showed that hexagonal and spherical in nature (Poedji Loekitowati Hariani et al., 2013).

Analysis of the SEM image of synthesized iron oxide nanoparticles showed a clear image of the nanoparticles ranges from 30 nm to 110 nm. However the percentage of nanoparticles beyond 100 nm is very less. The average percentage of nanoparticles present in the synthesized sample is 66 nm. From the image, it is confirmed that the sample contains various sizes of nanoparticles which are indeed agreement with the result obtained from DLS particle analyses (Behera et al., 2012). Cheng-Di et al., 2016 reported in his study, SEM observations of the nanoparticles indicated that the nano-scale zero valent iron (nZVI) formed small spherical particles, indicating a high degree of

nanoparticle dispersion. The SEM image of the particles revealed the average diameter of maghemite nanoparticles synthesized in the study around 45nm (Abbas Afkhami et al., 2009).

3.2.3 X-ray Diffraction (XRD)

The structural characterizations of the prepared Fe_2O_3 nanoparticles were carried out by using X–ray diffraction pattern analysis. The X–ray diffraction patterns were shown in Fig. 3.5 from which it was clear that the samples were crystalline in nature. The peaks appeared at 2θ of 31.8596, 45.5656, 56.7600 and 75.3720 Cross ponding to their respective (012), (110), (113) and (220) Miller planes. From the X–ray diffraction analysis it was observed that samples belong to the alpha (α) phase of iron oxide (JCPDS card number 33–0664) which has rhombohedral structure. The crystallite size has been calculated using X– ray diffraction data by employing Scherrer's equation. The average crystallite size was found to be of the order of 53.83 nm.

$$Particle\ Size = (0.9 \times \lambda)/(d \cos\theta)$$

Where 0.9 is a dimension constant of the equipment, λ is the wavelength of radiation corresponding of the Cu Kα, peak and θ is the Bragg's angle.

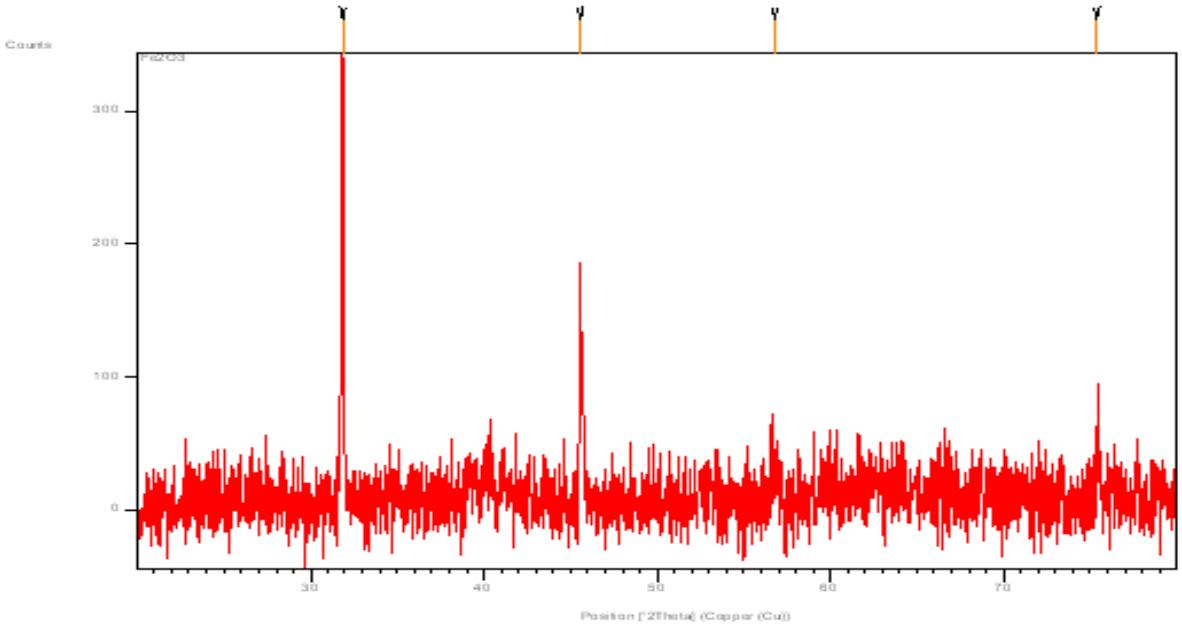

Figure 3.5. X–ray diffraction analysis of synthesized NPs.

Study conducted by Baalousha, 2008 revels that the crystallographic structure of the synthesized particles was determined by XRD and found to be pure iron oxide/hydroxide, poor crystalline nano-scale hematite particles (Fe_2O_3).

Study conducted by Cheng-Di et al., 2016 reported that XRD spectra were used to characterize the phase structure of the nano-scale zero valent iron (nZVI) nanostructures. The broad peak reveals the existence of an amorphous phase of iron. The characteristic peak at $2\theta = 44.9°$ confirmed the presence of fresh nZVI the magnetic hysteresis loops of fresh nZVI with a magnetic field cycle between −10 and +10 kOe at 300 K.

The XRD pattern of Fe-nanocomposite clearly show that the crystallites in the catalyst mainly consist of Fe_2O_3 (maghemite) and $Fe_2Si_4O_{10}(OH)_2$ (iron silicate hydroxide) (Jiyun Feng et al., 2003).

The XRD profile of maghemite nanoparticles shows that the calculated size of crystallite measured to be around 8.78nm according to scherrer equation. The peak at angle θ of 1.5418 (Abbas Afkhami et al., 2009).

The XRD patterns depict different iron oxide with five characteristic peaks at $2\theta = 30.5^o$, 35.5^o, 43.1^o, 57.0^o, and 62.6^o, corresponding to the crystal planes of (220), (311), (400), (511), and (440). The average crystallite size calculated using the Debye Scherrer equation was found to be 25 nm (Bedabrata Saha et al., 2010).

The XRD pattern showing 2θ=24.140, 33.140, 35.610, 40.840, 49.450, 54.060, 62.420, and 64.000. The peaks found in the angle are lapelled as (0,1,2), (1,0,4), (1,1,0), (1,1,3), (0,2,4) ,(1,1,6) planes per the JCPDS.NO.89-8104 file. The geometry of the Iron Oxide nanoparticles found as per this XRD data corresponds to rhombohedra geometry (K.Tharani, L.C. Nehru, 2015).

3.3 Analysis of Dye Solutions Treated by Nanoparticles

3.3.1 pH

pH for Red, Blue, Yellow and Mix dye before the experiment was found to be 3.7, 5.0, 5.6 and 7.1 respectively. After vigorous stirring of the dye solutions with nanoparticles for 30mins, considerable decolourization was noticed after settling of

nanoparticles at the bottom. For 5% dye solution of Red dye pH was decreased to 3.5. In all other solutions pH Increase was noticed. After treatment with nanoparticles, the pH for 5% dye solution of Blue azo reactive was increased from 5.0 to 7.9. The readings for 5% dye solutions were 3.5 for Red, 7.9 for Yellow and 8.1 for Mix and the readings for 10% dye solutions were 6.3 for Red, 7.3 for Blue and 7.9 for Yellow respectively.

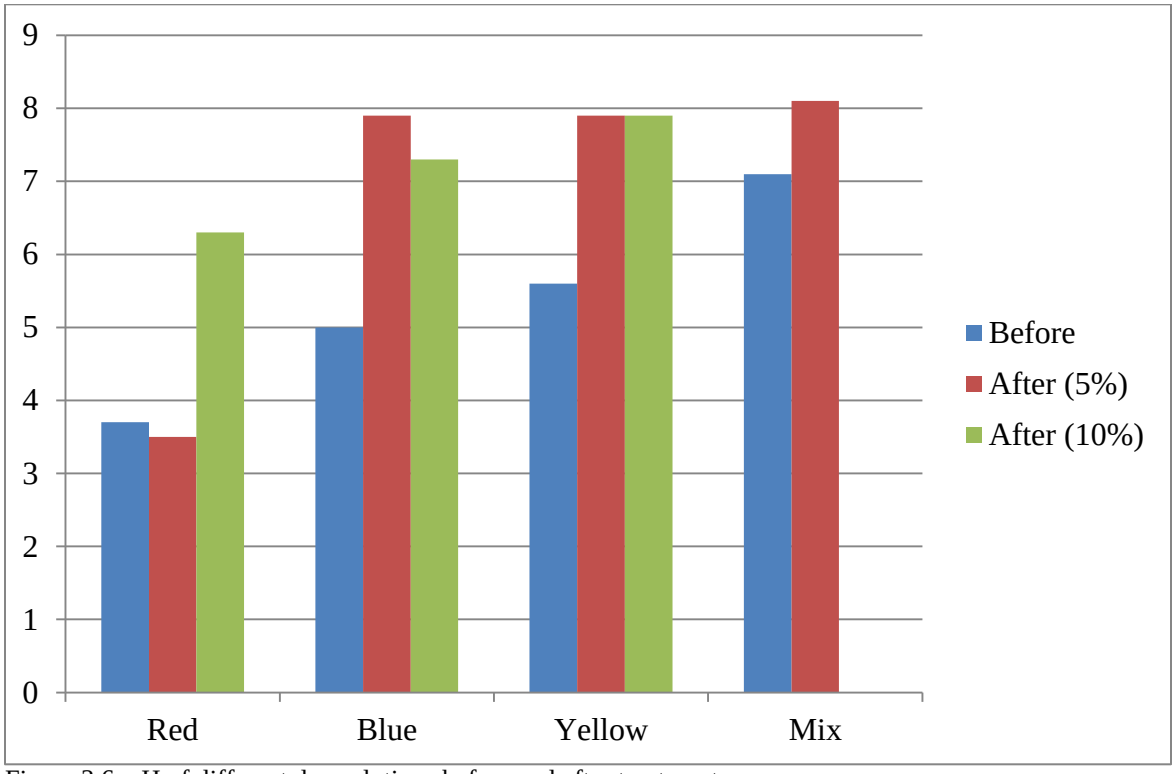

Figure 3.6. pH of different dye solutions before and after treatment.

The total change in pH in case of Red dye solutions was -5.4% for 5% solution and 70.27% for 10% solution. While for Blue dye solutions was 58% for 5% solution and 46% for 10% solution. For Yellow dye solutions was 41.07% for 5% solution and 10% solution respectively. And for Mix dye solution was 14.08%.

The result indicated that iron oxide nanoparticles was effective to reduce the colour, pH, electrical conductivity COD and calcium chemically synthesized iron nanoparticles can be used for the removal of contaminants present in the textile dyeing industry effluent.

Iron oxide nanoparticles show varied activity under varying pH conditions. In one study, it was found that hematite nanoparticles with smaller diameters are more active at low pH conditions as compared to larger diameter particles (Madden et al. 2006).

Many studies have revealed that the solution pH can dramatically influence the photo assisted Fenton degradation of organic compounds and the optimal solution pH is determined to be about 3.0 (Jiyun Feng et al., 2003).

The effect of pH in the range 4.0 to 7.6 on the removal of Congo Red was investigated using $0.01 molL^{-1}$ HCl or NaOH solution for pH adjustment. The percentage absorption increased by increasing pH and reached maximum at pH 5.9 and decreased at higher pHs. At higher pHs. The high negatively charged adsorbent surface sites did not favour the adsorption of deprotonated Congo Red due to electrostatic repulsion (Abbas Afkhami et al., 2009).

3.3.2 Total Dissolved Solids (TDS)

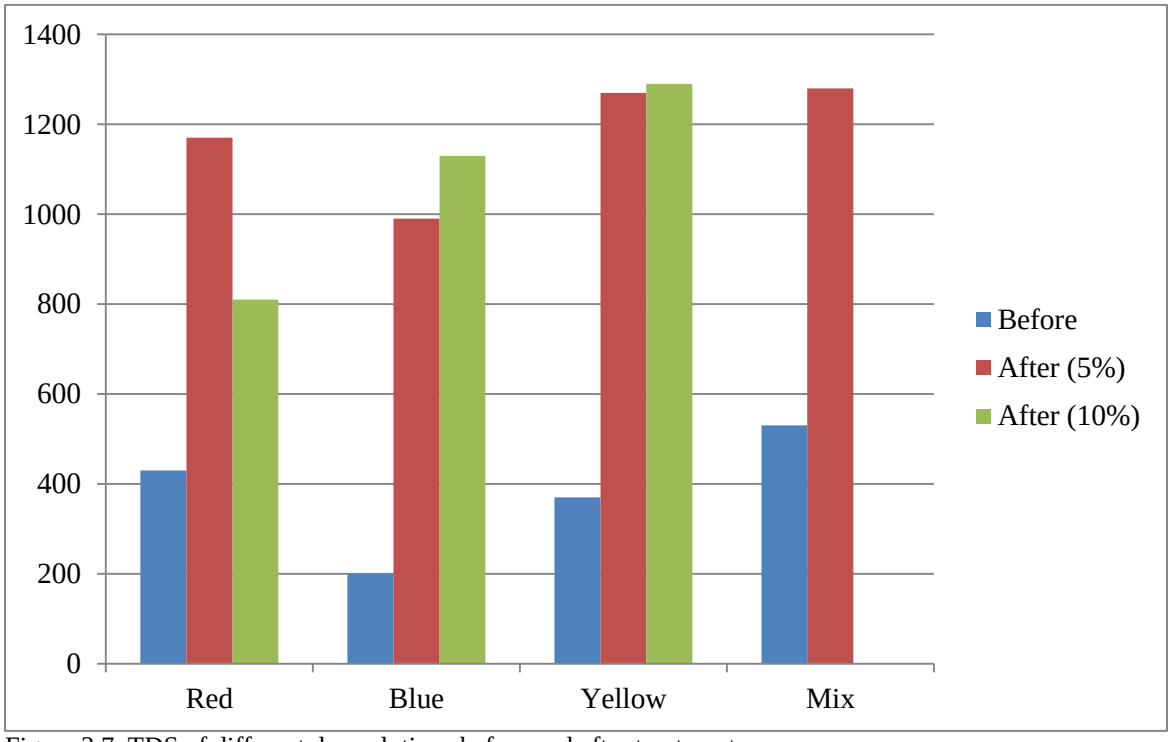

Figure 3.7. TDS of different dye solutions before and after treatment.

TDS for Red, Blue, Yellow and Mix dye before the experiment was found to be 430, 200, 370 and 530 respectively. After the experiment it was found that TDS was

increased after addition of nanoparticles. For 5% dye solutions total dissolved solids were increased to 1170, 990, 1270 and 1280 and for 10% dye solutions total dissolved solids were increased to 810, 1130 and 1290 respectively.

Some of the increase in TDS accounts for the addition of nanoparticles and also because of the presence of degraded products of azo reactive dyes in the mixture. The presence of nanoparticles cannot be judged by the naked eye as they were very small in size. To decrease the TDS it was required to pass the sample through nano-filter.

3.3.3 Electrical Conductivity (EC)

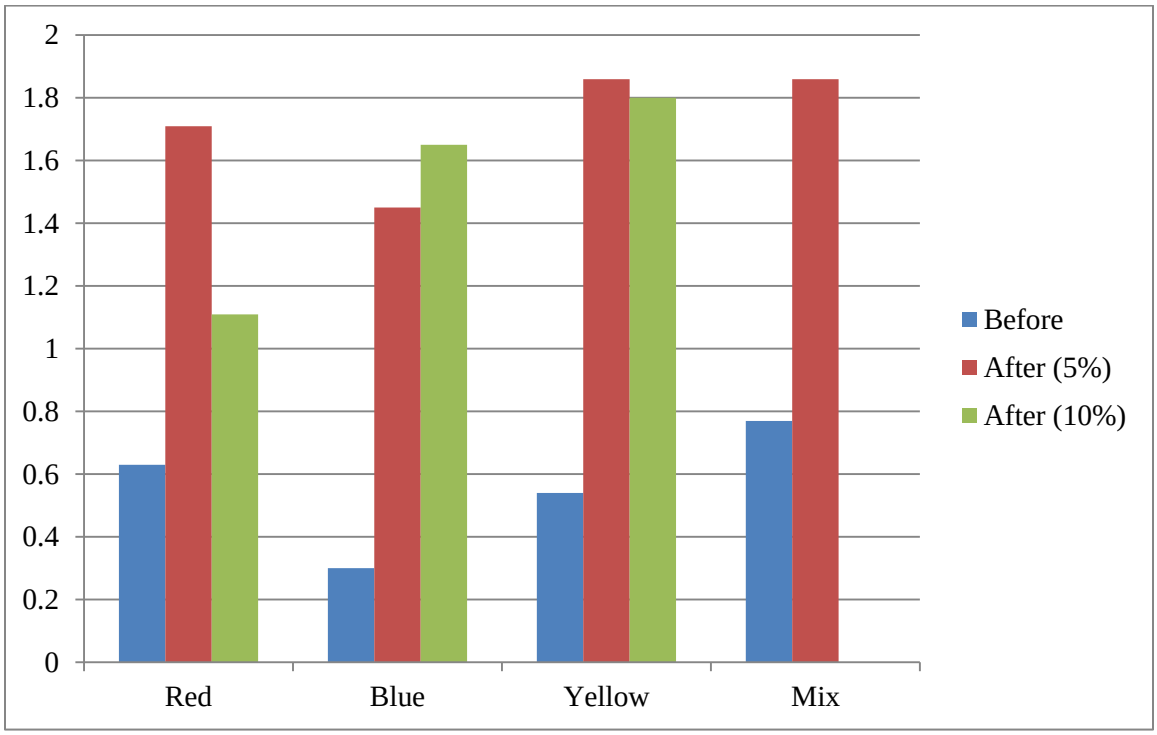

Figure 3.8. EC of different dye solutions before and after treatment.

Before the experiment Electrical Conductivity values for Red, Blue, Yellow and Mix dye solutions were measured to be 0.63, 0.3, 0.54 and 0.77 respectively. After the experiment it was found that EC was increased. For 5% dye solutions were 1.71, 1.45, 1.86 and 1.86 and for 10% dye solutions were 1.11, 1.65 and 1.8 respectively.

Some of the increase in EC accounts for the addition of nanoparticles and also because of the presence of degraded products of azo reactive dyes in the mixture. EC can also be reduced by passing the sample through nano-filter.

3.3.4 Chemical Oxygen Demand (COD)

Before the experiment Chemical Oxygen Demand values for Red, Blue, Yellow and Mix dye solutions were measured. For 5% dye solutions were 810, 750, 1125 and 1860. And for 10% dye solutions were 1520, 1435 and 1780 as there was no mix dye solution in 10%. After the experiment it was found that COD was decreased. For 5% dye solutions were 590, 490, 625 and 1190 and for 10% dye solutions were 1080, 980 and 1120 respectively.

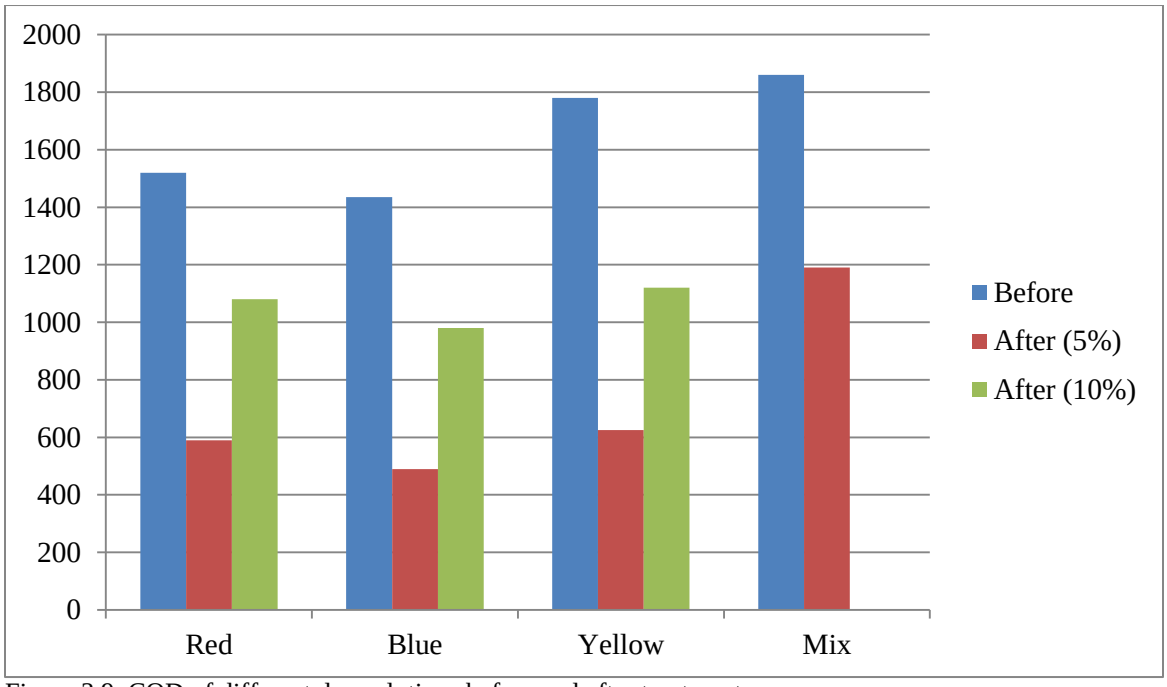

Figure 3.9. COD of different dye solutions before and after treatment.

There was a decrease in COD concentration recorded after experiment. However the least effect was recorded in Mix dye solution where the decrease in concentration was very less as compare to other solutions.

3.3.5 Decolourisation

UV absorbance values before treatment with nanoparticles for Red dye it was 3.0, for Yellow it was 3.0, for Blue dye it was 1.54 and for Mix dye it was 1.06. After experimentation it was found that decolourization occurred and the results for 5% dye solutions were 0.037 for Red, 0.004 for Blue, 0.028 for Yellow and 0.04 for Mix and for 10% dye solutions were 0.099 for Red, 0.01 for Blue and 0.009 for Yellow respectively.

In the present research, significant decolourization was observed. Efficiency of Decolourization in case of Red dye solutions was 98.76% for 5% solution and 96.7% for 10% solution. For Blue dye solutions was 99.74% for 5% solution and 99.35% for 10% solution. For Yellow dye solutions was 99.06% for 5% solution and 99.7% for 10% solution. And for Mix dye solution was 96.23%.

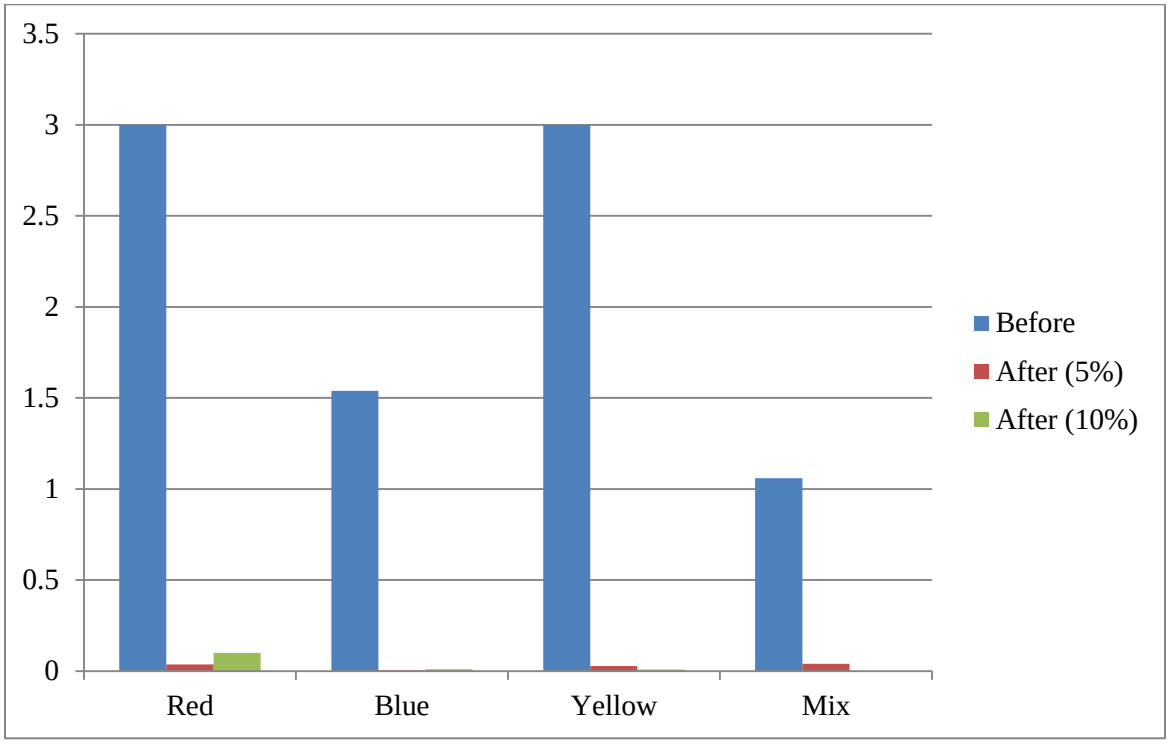

Figure 3.10. UV absorbance of different dye solutions before and after treatment.

Kale et al (2014) reported the decolourization of dye using nickel nanoparticles. Fan et al (2009) also reported the rapid decolourization of azo dye methyl orange in aqueous solution by nanoscale zerovalent iron particles. From the present study, the physico-chemical parameters were reduced with increasing dose of iron oxide nanoparticles.

3.4 Effect of pH on Treatment

3.4.1 Effect of Acidic Conditions 3pH and 5pH

pH for Red, Blue, Yellow and Mix dye before treatment was fixed at 3 and 5 by using concentrated HCl.

3.4.1.1 Total Dissolved Solids of 3pH Dye Solutions

TDS for Red, Blue, Yellow and Mix dye before the experiment was found to be 430, 200, 370 and 530 respectively. After the experiment it was found that TDS was increased. The readings were 1510, 1120, 1030 and 1500 respectively.

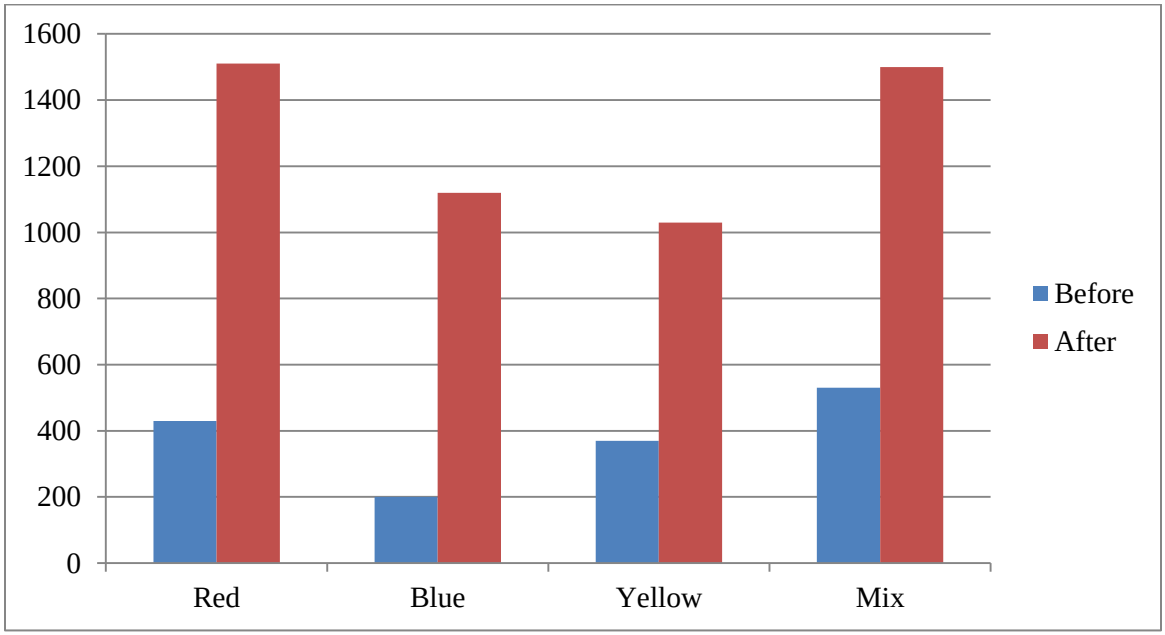

Figure 3.11. TDS of different dye solutions of 3pH variable before and after treatment.

3.4.1.2 Electrical Conductivity of 3pH Dye Solutions

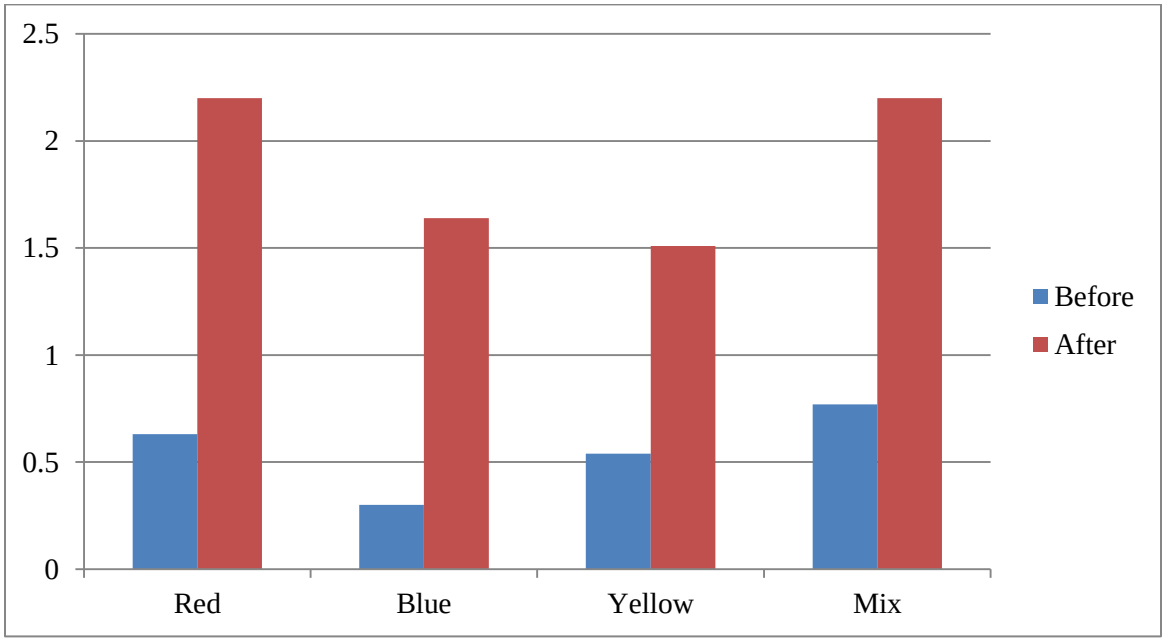

Figure 3.12. EC of different dye solutions of 3pH variable before and after treatment.

Before the experiment Electrical Conductivity values for Red, Blue, Yellow and Mix dye solutions were measured to be 0.63, 0.3, 0.54 and 0.77 respectively. After the experiment it was found that EC was increased. The readings were 2.2, 1.64, 1.51 and 2.2 respectively.

3.4.1.3 Chemical Oxygen Demand of 3pH Dye Solutions

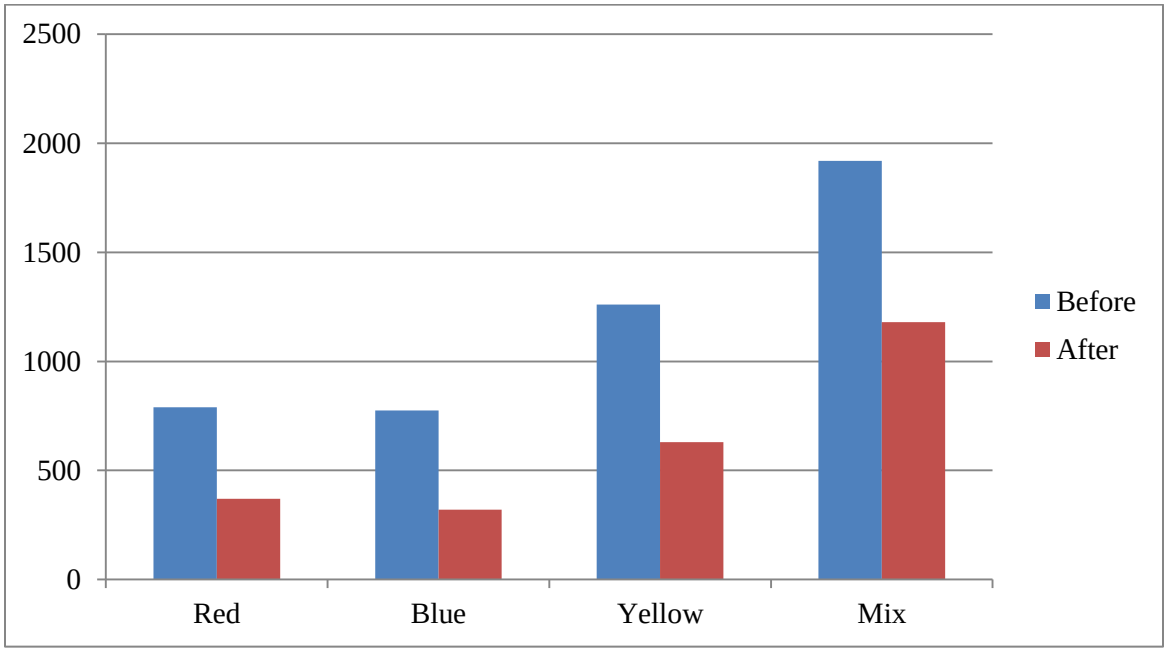

Figure 3.13. COD of different dye solutions of 3pH variable before and after treatment.

Before the experiment Chemical Oxygen Demand values for Red, Blue, Yellow and Mix dye solutions were measured to be 790, 775, 1260 and 1920 respectively. After the experiment it was found that COD was decreased. The readings were 370, 320, 630 and 1180 respectively.

3.4.1.4 Decolourisation of 3pH Dye Solutions

UV absorbance values before the experiment were 3 for Red and Yellow dye solutions, 1.54 for Blue dye solution and 1.06 for Mix dye solution. After experimentation it was found that massive decolourization was occurred and for Red was 0.01, for Blue was 0.097, for Yellow was 0.032 and for Mix dye solution was 0.148.

Efficiency of decolourization for Red dye solution was 99.66%, for Blue dye solution was 93.70%, for Yellow dye solution was 98.93% and for Mix dye solution was 86.04%.

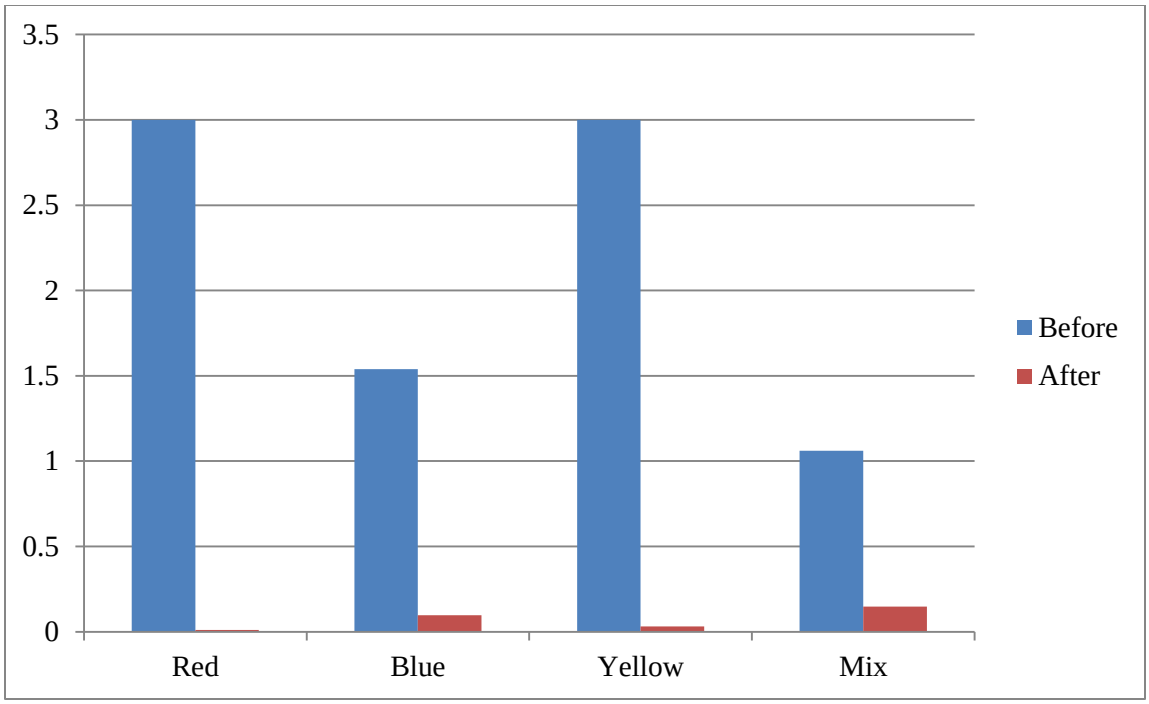

Figure 3.14. UV absorbance of different dye solutions of 3pH variable before and after treatment.

3.4.1.5 Total Dissolved Solids of 5pH Dye Solutions

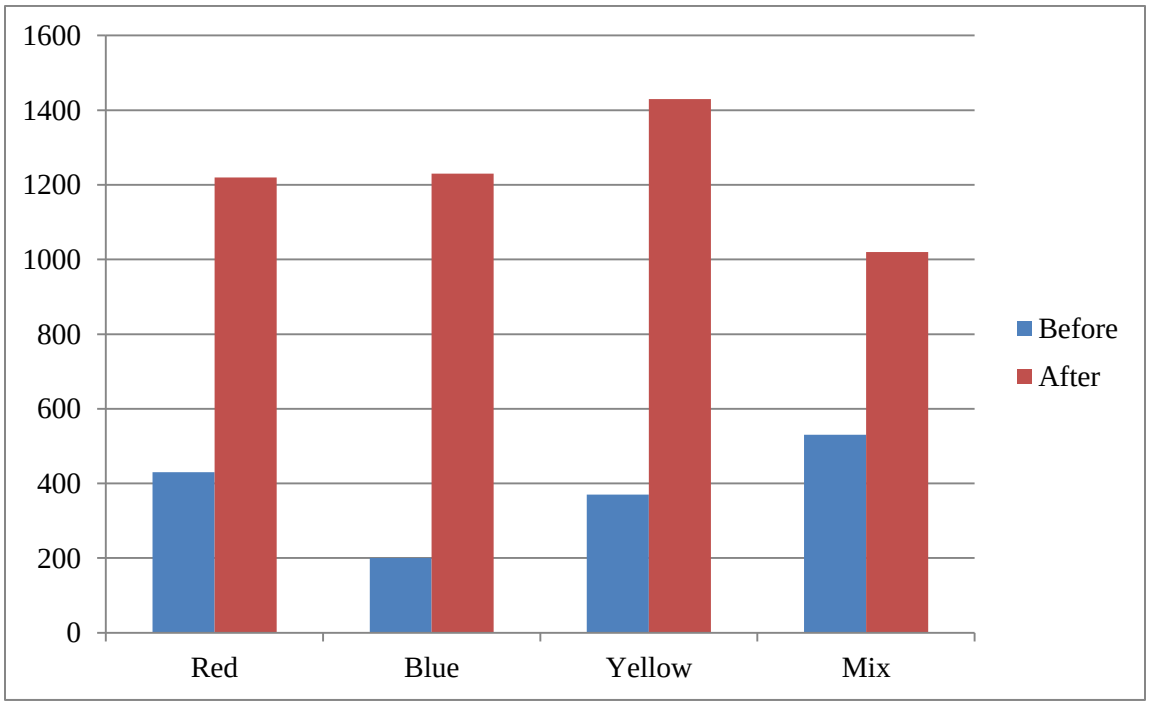

Figure 3.15. TDS of different dye solutions of 5pH variable before and after treatment.

TDS for Red, Blue, Yellow and Mix dye at before the experiment was found to be 430, 200, 370 and 530 respectively. After the experiment it was found that TDS was increased. The readings were 1220, 1230, 1430 and 1020 respectively.

3.4.1.6 Electrical Conductivity of 5pH Dye Solutions

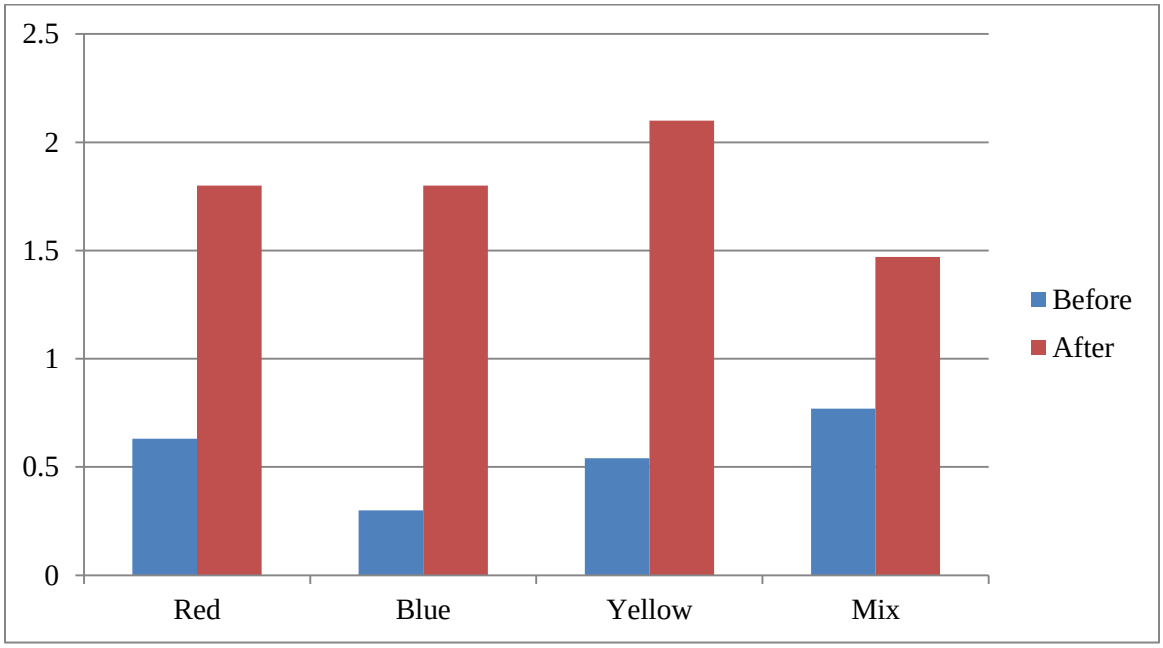

Figure 3.16. EC of different dye solutions of 5pH variable before and after treatment.

Before the experiment Electrical Conductivity values for Red, Blue, Yellow and Mix dye solutions were measured to be 0.63, 0.3, 0.54 and 0.77 respectively. After the experiment it was found that EC was increased. The readings were 1.8, 1.8, 2.1 and 1.47 respectively.

3.4.1.7 Chemical Oxygen Demand of 5pH Dye Solutions

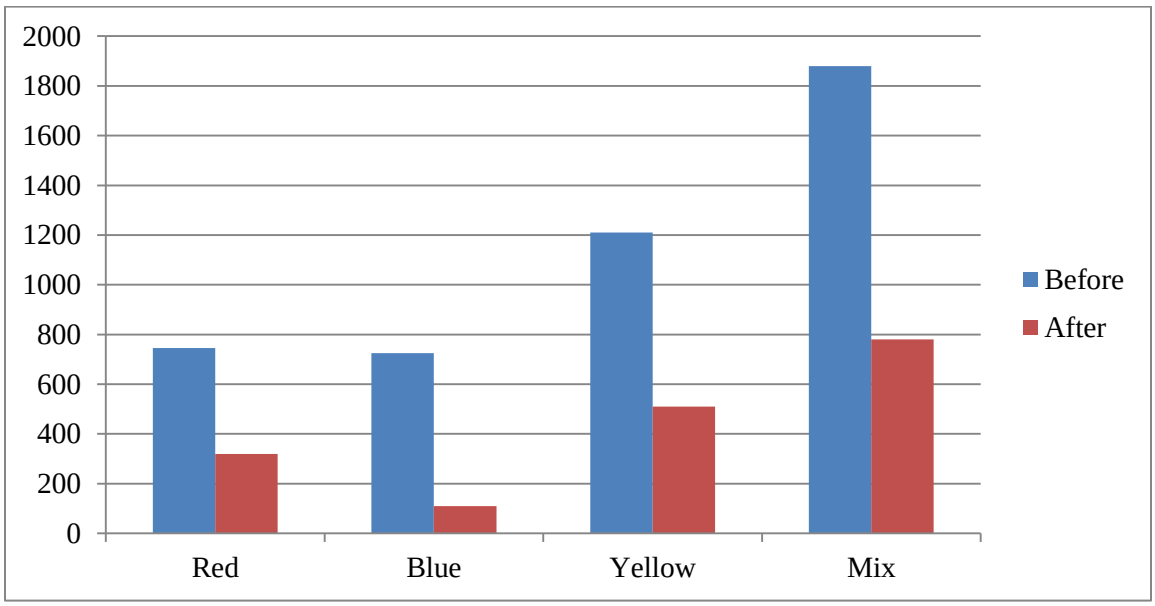

Figure 3.17. COD of different dye solutions of 5pH variable before and after treatment.

Before the experiment Chemical Oxygen Demand values for Red, Blue, Yellow and Mix dye solutions were measured to be 745, 725, 1210 and 1880 respectively. After the experiment it was found that COD was decreased. The readings were 320, 110, 510 and 780 respectively.

3.4.1.8 Decolourisation of 5pH Dye Solutions

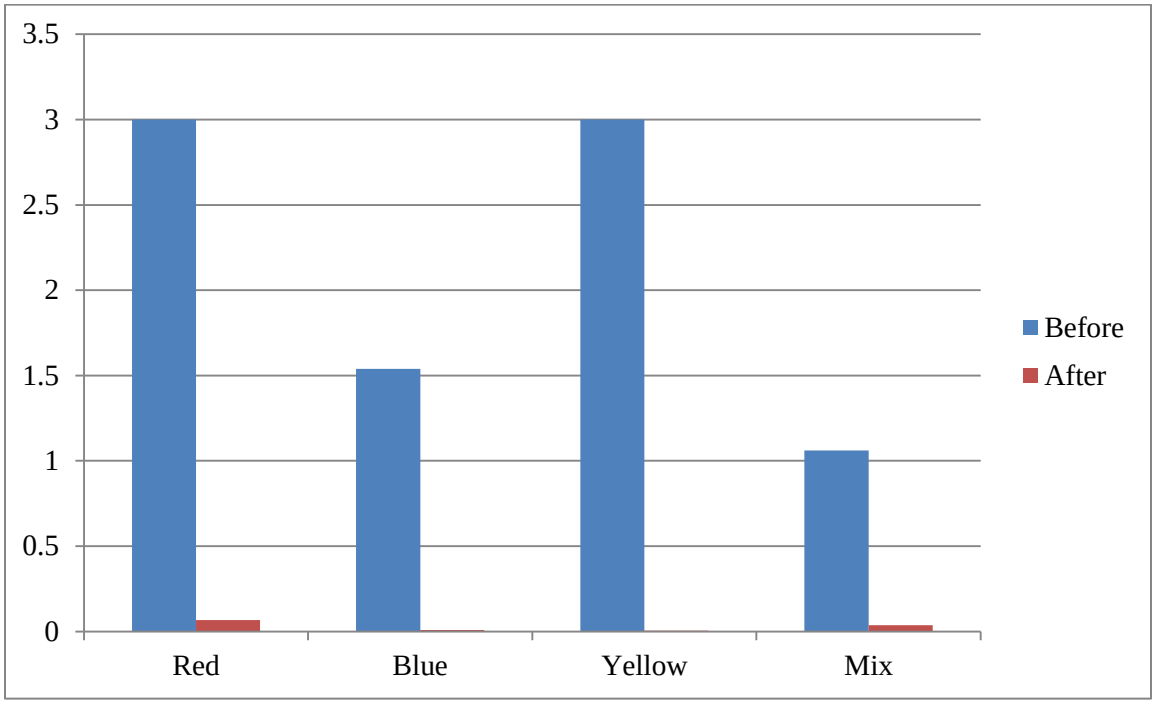

Figure 3.18. UV absorbance of different dye solutions of 5pH variable before and after treatment.

UV absorbance for Red, Blue, Yellow and Mix dye before the experiment was found to be 3, 1.54, 3 and 1.06 respectively. After the experiment it was found that massive decolourization was occurred. The readings were 0.066, 0.009, 0.005 and 0.036 respectively.

Efficiency of decolourization for Red dye solution was 97.80%, 99.42% for Blue dye solution, 99.83% for Yellow dye solution and 96.60% for Mix dye solution.

3.4.2 Effect of Basic Conditions 9 and 11

pH for Red, Blue, Yellow and Mix dye before the experiment was fixed at 9 and 11 by using concentrated NaOH.

3.4.2.1 Total Dissolved Solids of 9pH Dye Solutions

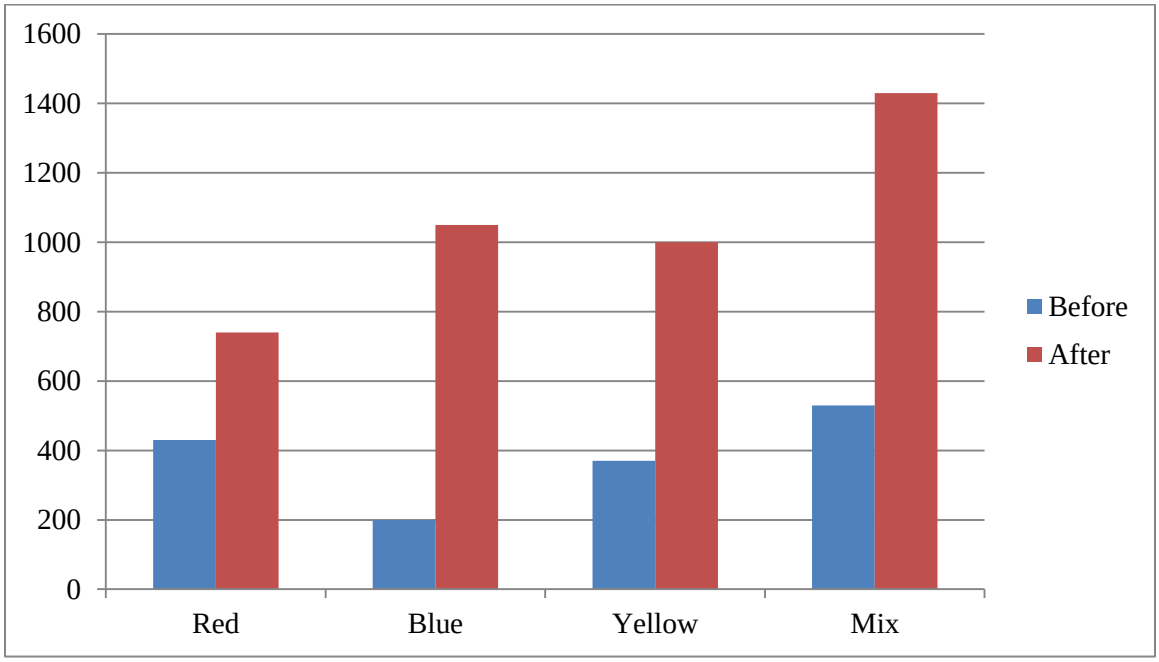

Figure 3.19. TDS of different dye solutions of 9pH variable before and after treatment.

TDS for Red, Blue, Yellow and Mix dye before the experiment was found to be 430, 200, 370 and 530 respectively. After the experiment it was found that TDS was increased. The readings were 740, 1050, 1000 and 1430 respectively.

3.4.2.2 Electrical Conductivity of 9pH Dye Solutions

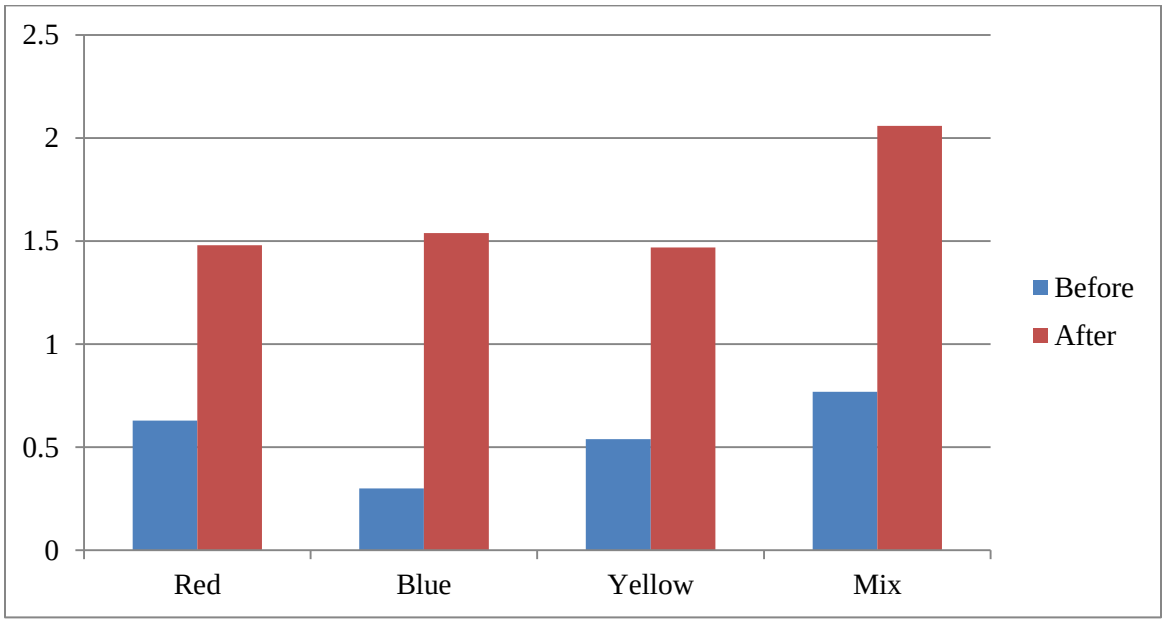

Figure 3.20. EC of different dye solutions of 9pH variable before and after treatment.

Before the experiment Electrical Conductivity values for Red, Blue, Yellow and Mix dye solutions were measured to be 0.63, 0.3, 0.54 and 0.77 respectively. After the experiment it was found that EC was increased. The readings were 1.48, 1.54, 1.47 and 2.06 respectively.

3.4.2.3 Chemical Oxygen Demand of 9pH Dye Solutions

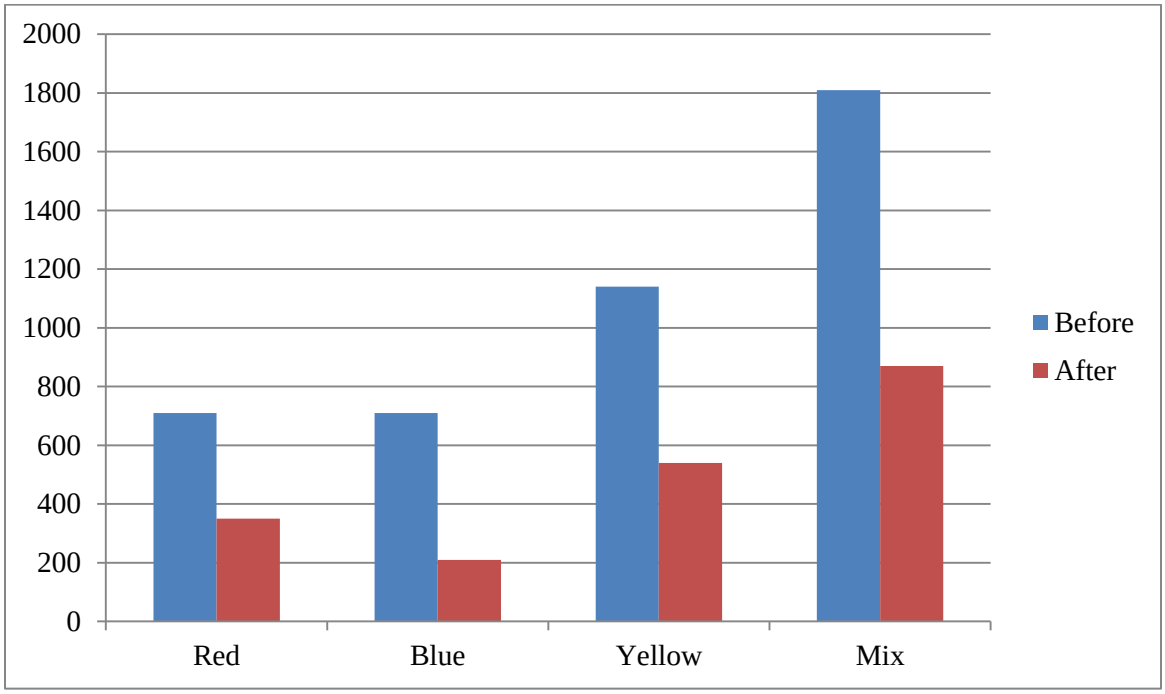

Figure 3.21. COD of different dye solutions of 9pH variable before and after treatment.

Before the experiment Chemical Oxygen Demand values for Red, Blue, Yellow and Mix dye solutions were measured to be 710, 710, 1140 and 1810 respectively. After the experiment it was found that COD was decreased. The readings were 350, 210, 540 and 870 respectively.

3.4.2.4 Decolourisation of 9pH Dye Solutions

UV absorbance for Red, Blue, Yellow and Mix dye before the experiment was found to be 3, 1.54, 3 and 1.06 respectively. After the experiment it was found that massive decolourization was occurred. The readings were 0.162, 0.031, 0.145 and 0.120 respectively.

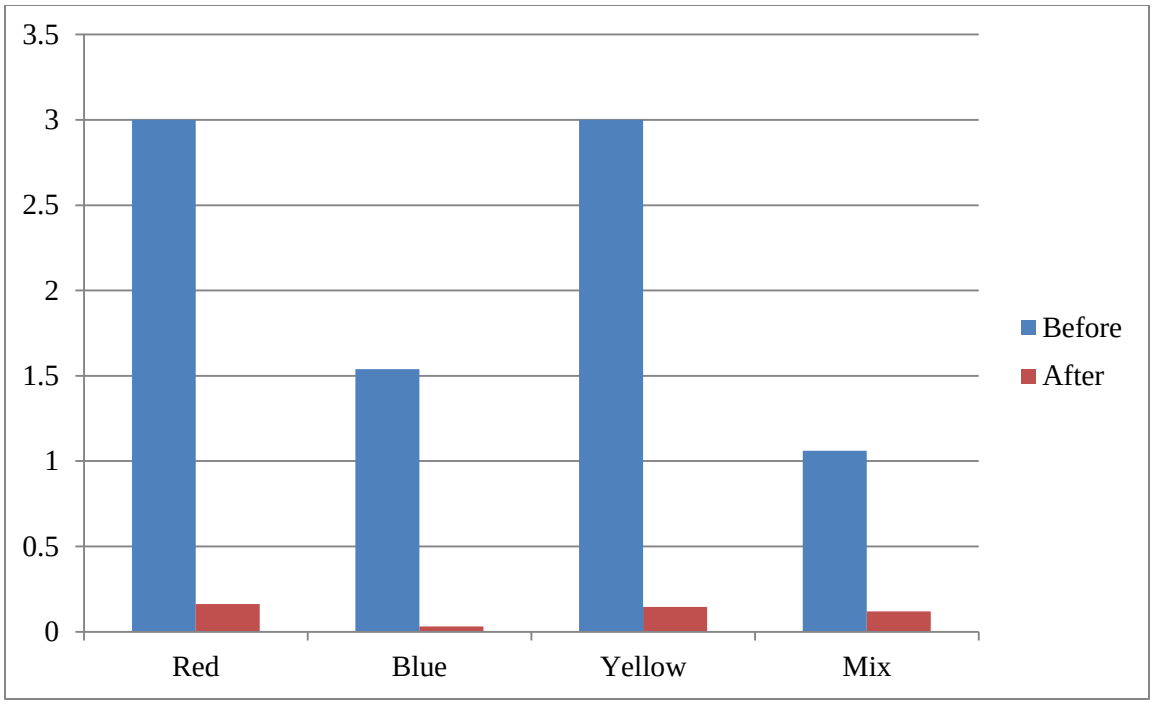

Figure 3.22. UV absorbance of different dye solutions of 9pH variable before and after treatment.

Efficiency of decolourization for Red dye solution was 94.6%, for Blue dye solution was 97.99%, for Yellow dye solution was 95.16% and for Mix dye solution was 88.68%.

3.4.2.5 Total Dissolved Solids of 11pH Dye Solutions

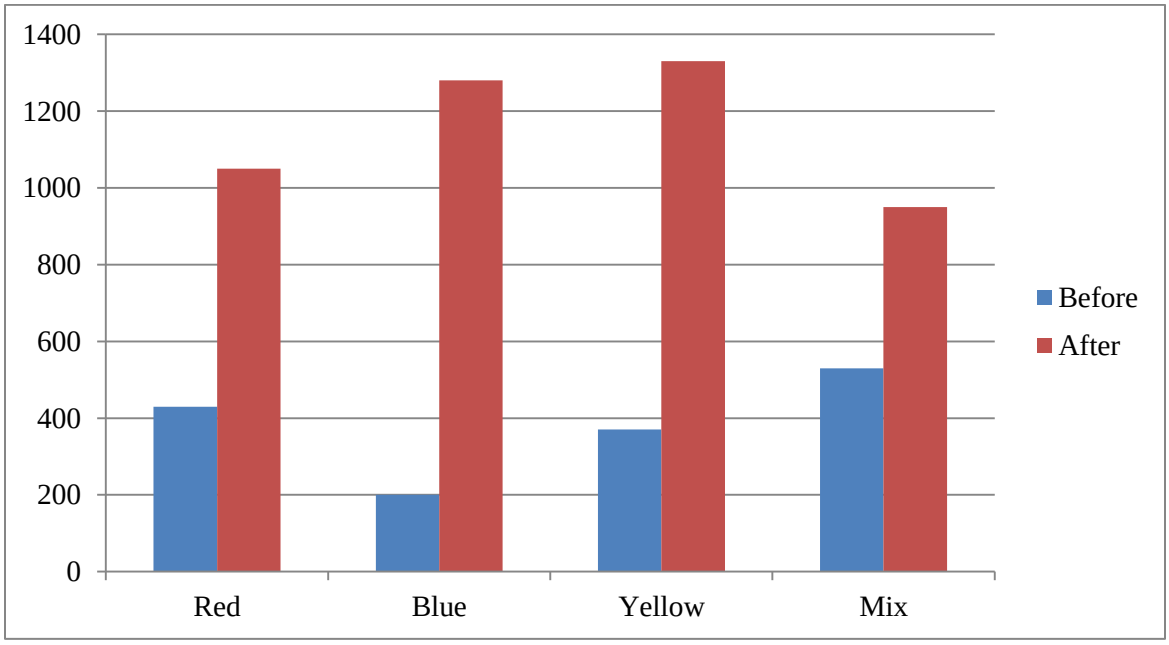

Figure 3.23. TDS of different dye solutions of 11pH variable before and after treatment.

TDS for Red, Blue, Yellow and Mix dye before the experiment was found to be 430, 200, 370 and 530 respectively.

After the experiment it was found that TDS was increased. The readings were 1050, 1280, 1330 and 950 respectively.

3.4.2.6 Electrical Conductivity of 11pH Dye Solutions

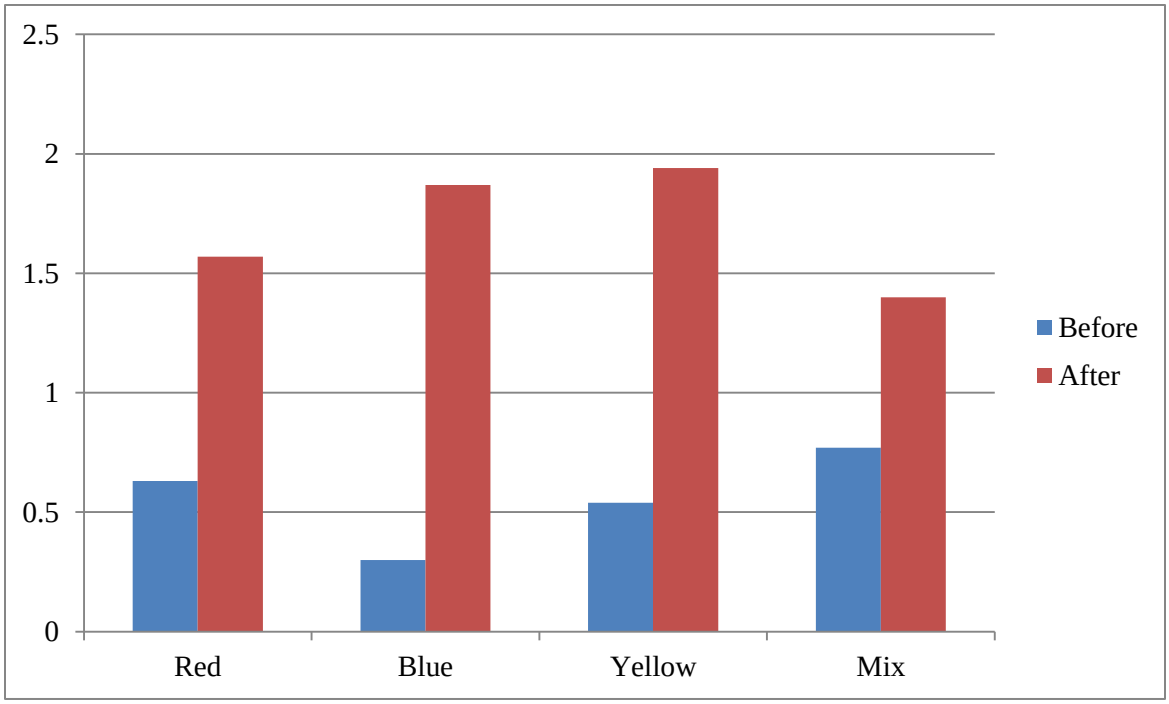

Figure 3.24. EC of different dye solutions of 11pH variable before and after treatment.

Before the experiment Electrical Conductivity values for Red, Blue, Yellow and Mix dye solutions were measured to be 0.63, 0.3, 0.54 and 0.77 respectively. After the experiment it was found that EC was increased. The readings were 1.57, 1.87, 1.94 and 1.4 respectively.

3.4.2.7 Chemical Oxygen Demand of 11pH Dye Solutions

Before the experiment Chemical Oxygen Demand values for Red, Blue, Yellow and Mix dye solutions were measured to be 730, 730, 1180 and 1850 respectively. After the experiment it was found that COD was decreased. The readings were 440, 590, 970 and 1330 respectively.

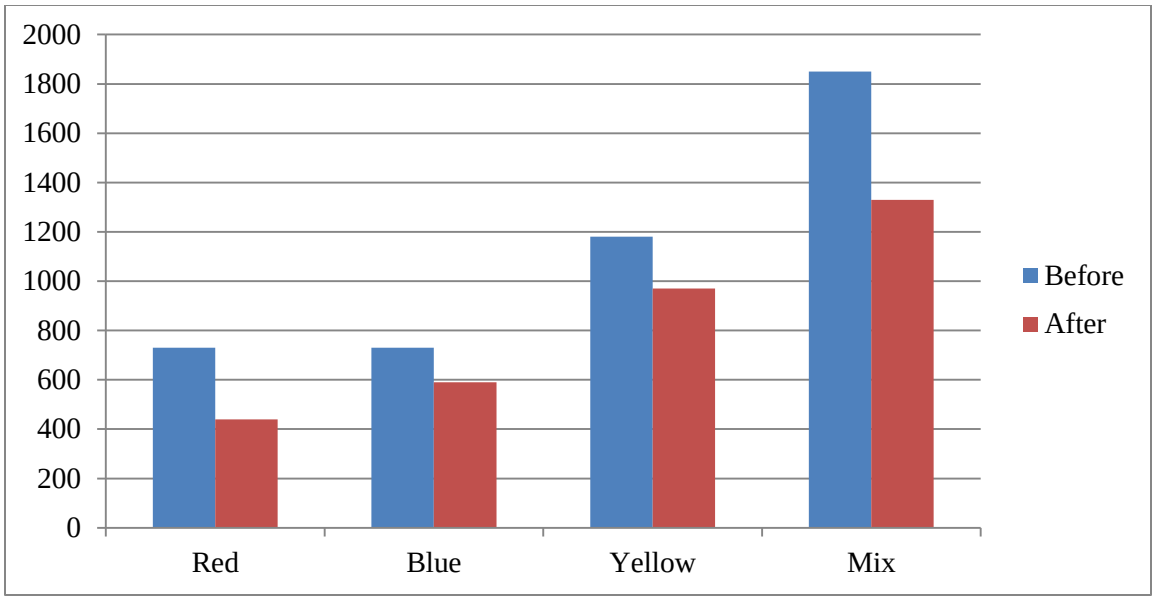

Figure 3.25. COD of different dye solutions of 11pH variable before and after treatment.

3.4.2.8 Decolourisation of 11pH Dye Solutions

UV absorbance for Red, Blue, Yellow and Mix dye before the experiment was found to be 3, 1.54, 3 and 1.06 respectively. After the experiment it was found that massive decolourization was occurred. The readings were 0.607, 0.103, 0.336 and 0.719 respectively.

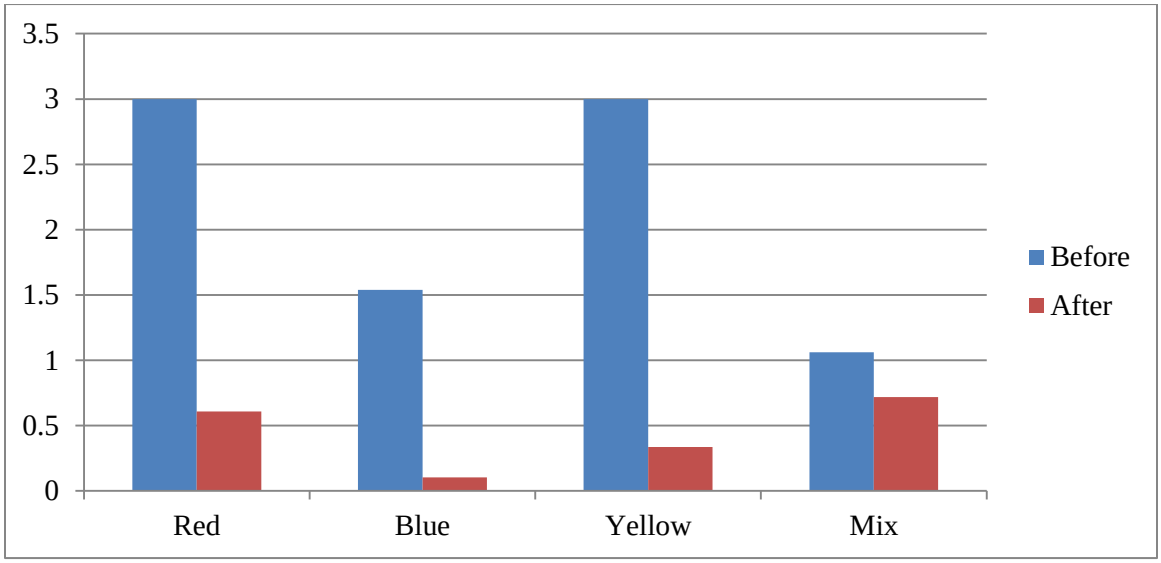

Figure 3.26. UV absorbance of different dye solutions of 11pH variable before and after treatment.

Efficiency of decolourization for Red dye solution was 79.76%, for Blue dye solution was 93.31%, for Yellow dye solution was 88.80% and for Mix dye solution was 32.17%.

Table 3.1. Comparison of results before and after treatment of Dyes Solutions based on percentage.

	Concen-tration	COD Mg/l		pH		EC Ms/cm		TDS ppm		UV Abs	
		Before	**After**	**Before**	**After**	**Before**	**After**	**Before**	**After**	**Before**	**After**
Red	5%	810	590	3.7	3.5	0.63	1.71	430	1170	3.0	0.037
Blue	5%	750	490	5.0	7.9	0.30	1.45	200	990	1.54	0.004
Yellow	5%	1125	625	5.6	7.9	0.54	1.86	370	1270	3.0	0.028
Red	10%	1520	1080	3.7	6.3	0.63	1.11	430	810	3.0	0.099
Blue	10%	1435	980	5.0	7.3	0.30	1.65	200	1130	1.54	0.010
Yellow	10%	1780	1120	5.6	7.9	0.54	1.80	370	1290	3.0	0.009
Mix	5%+5%+ 5%	1860	1190	7.1	8.1	0.77	1.86	530	1280	1.06	0.040

Table 3.2. Comparison of results before and after treatment of Dyes Solution of 3pH.

	Concen-tration	COD Mg/l		pH		EC Ms/cm		TDS ppm		UV Abs	
		Before	**After**	**Before**	**After**	**Before**	**After**	**Before**	**After**	**Before**	**After**
Red	5%	790	370	3	7.3	0.63	2.20	430	1510	3.0	0.010
Blue	5%	775	320	3	3.3	0.30	1.64	200	1120	1.54	0.097
Yellow	5%	1260	630	3	5.2	0.54	1.51	370	1030	3.0	0.032
Mix	5%+5%+ 5%	1920	1180	3	3.7	0.63	2.20	430	1500	3.0	0.148

Table 3.3. Comparison of results before and after treatment of Dyes Solution of 5pH.

	Concen-tration	COD Mg/l		pH		EC Ms/cm		TDS ppm		UV Abs	
		Before	**After**	**Before**	**After**	**Before**	**After**	**Before**	**After**	**Before**	**After**
Red	5%	745	320	5	7.1	0.63	1.80	430	1220	3.0	0.066
Blue	5%	725	110	5	8.0	0.30	1.80	200	1230	1.54	0.009
Yellow	5%	1210	510	5	5.6	0.54	2.10	370	1430	3.0	0.005
Mix	5%+5%+ 5%	1880	780	5	5.8	0.63	1.47	430	1020	3.0	0.036

Table 3.4. Comparison of results before and after treatment of Dyes Solution of 9pH.

	Concen-tration	COD Mg/l		pH		EC Ms/cm		TDS ppm		UV Abs	
		Before	**After**	**Before**	**After**	**Before**	**After**	**Before**	**After**	**Before**	**After**
Red	5%	710	350	9	7.3	0.63	1.48	430	0740	3.0	0.162
Blue	5%	710	210	9	6.4	0.30	1.54	200	1050	1.54	0.031
Yellow	5%	1140	540	9	7.0	0.54	1.47	370	1000	3.0	0.145
Mix	5%+5%+ 5%	1810	870	9	6.5	0.63	2.06	430	1430	3.0	0.120

Table 3.5. Comparison of results before and after treatment of Dyes Solution of 11pH.

	Concen-tration	COD Mg/l		pH		EC Ms/cm		TDS ppm		UV Abs	
		Before	**After**	**Before**	**After**	**Before**	**After**	**Before**	**After**	**Before**	**After**
Red	5%	730	440	11	8.7	0.63	1.57	430	1050	3.0	0.607
Blue	5%	730	590	11	8.8	0.30	1.87	200	1280	1.54	0.103
Yellow	5%	1180	970	11	8.7	0.54	1.94	370	1330	3.0	0.336
Mix	5%+5%+ 5%	1850	1330	11	7.5	0.63	1.40	430	0950	3.0	0.719

CONCLUSIONS

1. Synthesized nanoparticles were very effective in removal of azo reactive dyes.
2. XRD, SEM and FTIR of synthesized nanoparticles reveal the rhombohedral structural morphology with average size of 53.83nm.
3. Acidic conditions proved to be more suitable for removal of azo reactive dyes when treated with iron oxide nanoparticles.

RECOMMENDATIONS

1. Further research should be conducted in different temperature conditions.
2. Effect of concentration and time of interaction should be evaluated.
3. Pilot scale study should be conducted to study effect of iron oxide nanoparticles in treatment of textile waste water.
4. Different nanoparticles should also be considered for treatment of azo dyes.

REFERENCES

Abdulraheem, G., Peter Obinna, N., Kasali Ademola, B., & Kasali Ademola, K. (2012). Photocatalytic Decolourization and Degradation of CI Basic Blue 41 Using TiO 2 Nanoparticles. Journal of Environmental Protection, 2012.

Abbas Afkhami, Razieh Moosavi, 2009. Adsorptive removal of Congo Red, a carcinogenic textile dye, from aqueous solutions by maghemite nanoparticles.

Ahmad, A., & Puasa, S. (2007). Reactive dyes decolourization from an aqueous solution by combined coagulation/micellar-enhanced ultrafiltration process. *Chemical Engineering Journal, 132*(1), 257-265.

Bedabrata Saha, Sourav Das, Jiban Saikia, and Gopal Das, 2010. Preferential and Enhanced Adsorption of Different Dyes on Iron Oxide Nanoparticles

Badruddoza, A., Tay, A., Tan, P., Hidajat, K., & Uddin, M. (2011). Carboxymethyl-β-cyclodextrin conjugated magnetic nanoparticles as nano-adsorbents for removal of copper ions: synthesis and adsorption studies. *Journal of hazardous materials, 185*(2), 1177-1186.

Behera,S.S., J.K.Patra., K. Pramanik., N. Panda and H. Thatoi.2012. Characterization and Evaluation of Antibacterial Activities of Chemically Synthesized Iron Oxide

Booth, G., Zollinger, H., McLaren, K., Sharples, W. G., & Westwell, A. (2000a). Dyes, general survey. *Ullmann's Encyclopedia of Industrial Chemistry*.

Booth, G., Zollinger, H., McLaren, K., Sharples, W. G., & Westwell, A. (2000b). Dyes, General Survey *Ullmann's Encyclopedia of Industrial Chemistry*: Wiley-VCH Verlag GmbH & Co. KGaA.

Cheng-Di, Chiu-Wen Chen and Chang-Mao Hung, 2016. Magnetic Nanoparticles and Their Heterogeneous Persulfate Oxidation Organic Compound Applications

Cherepy, NJ., Liston, DB., Lovejoy, JA., Deng, H., Zhang, ZJ. (1998). Ultrafast Studies of Photoexcited Electron Dynamics in ⌟- and ⌟-Fe2O3 Semiconductor Nanoparticles. J. Phys. Chem. B Vol. 102, pp. 770.

Chung, K. T., & Stevens, S. E. (1993). Degradation azo dyes by environmental microorganisms and helminths. *Environmental Toxicology and Chemistry, 12*(11), 2121-2132.

Cornell, RM., Schwertmann, U. (2003) The Iron Oxides-Structure, Properties, Reactions, Occurrences and Uses. Darmstadt: Wiley–VCH GmbH & Co. KGaA.

Correia, V. M., Stephenson, T., & Judd, S. J. (1994). Characterisation of textile wastewaters-a review. *Environmental technology, 15*(10), 917-929.

Dalali, N., Khoramnezhad, M., Habibizadeh, M., & Faraji, M. (2011). *Magnetic removal of acidic dyes from waste waters using surfactant-coated magnetite nanoparticles: optimization of process by Taguchi method.* Paper presented at the International conference on environmental and agriculture engineering IPCBEE, Singapore.

Dinesh, G. K., Anandan, S., & Sivasankar, T. (2015). Sonophotocatalytic treatment of Bismarck Brown G dye and real textile effluent using synthesized novel Fe (0)-doped TiO 2 catalyst. *RSC Advances, 5*(14), 10440-10451.

Fan., Y. Guo., J. Wang, and M. Fan.2009. Rapid decolorization of azo dye methyl orange

G.A. Umbuzeiro, H. Freeman, S.H. Warren, F. Kummrow, and L.D. Claxton, “Mutagenicity evaluation of the commercial product C.I. Disperse Blue 291 using different protocols of the Salmonella assay,” Food and Chemistry Toxicology, vol.43, pp.49-56, 2005.

G.B. Michaels and D.L. Lewis, “Sorption and toxicity of azo and triphenyl methane dyes to aquatic microbial populations,” Environmental Contaminants and Toxicology, vol. 34, pp. 323-330, 1985.

G. M. Shaul, R.J. Lieberman, C.R. Dempsey, K.A. Dostal, “Treatability of water soluble azo dyes by the activated sludge process,” Proceedings of the Industrial Wastes Symposia WPCF, pp.1-18, 1986.

Hawks, J., Wang, E. T., Cochran, G. M., Harpending, H. C., & Moyzis, R. K. (2007). Recent acceleration of human adaptive evolution. *Proceedings of the National Academy of Sciences, 104*(52), 20753-20758.

He, Y., Gao, J.-F., Feng, F.-Q., Liu, C., Peng, Y.-Z., & Wang, S.-Y. (2012). The comparative study on the rapid decolorization of azo, anthraquinone and triphenylmethane dyes by zero-valent iron. *Chemical Engineering Journal, 179*, 8-18.

Jensen, M. C. (1993). The modern industrial revolution, exit, and the failure of internal control systems. *the Journal of Finance, 48*(3), 831-880.

Jiyun Feng, Xijun Hu, and Po Lock Yue, 2003. Degradation of Azo-dye Orange II by a Photoassisted Fenton Reaction Using a Novel Composite of Iron Oxide and Silicate Nanoparticles as a Catalyst

J.K. Lin and Y.H. Wu, “Studies on the mechanism of methemoglobin formation induced by aminoazo compounds,” Biochemistry Pharmacology, vol. 22, pp. 1883-1891, 1973.

K.Tharani, L.C. Nehru “Synthesis and Characterization of Iron Oxide Nanoparticle by Precipitation Method by International Journal of Advanced Research in Physical Science (IJARPS)” Link: https://www.arcjournals.org/pdfs/ijarps/v2-i8/6.pdf

Kale, R. D., Prerana Kane and Namrata Phulaware .2014. Decolourization of C. I. Reactive Black 5 by PVP stabilized Nickel nanoparticles. International Journal of Engineering Science and Innovative Technology, 2:4060.

Khin, M. M., Nair, A. S., Babu, V. J., Murugan, R., & Ramakrishna, S. (2012). A review on nanomaterials for environmental remediation. *Energy & Environmental Science*, *5*(8), 8075-8109.

Kim, D., Zhang, Y., Voit, W., Rao, K., & Muhammed, M. (2001). Synthesis and characterization of surfactant-coated superparamagnetic monodispersed iron oxide nanoparticles. *Journal of Magnetism and Magnetic Materials*, *225*(1), 30-36.

Kirk-Othmer, Encyclopedia of Chemical Technology. 3rd ed, New York: Wiley-Inter Science, 1979, pp. 1-172.

Laurent, S., Forge, D., Port, M., Roch, A., Robic, C., Vander Elst, L., & Muller, R. N. (2008). Magnetic iron oxide nanoparticles: synthesis, stabilization, vectorization, physicochemical characterizations, and biological applications. *Chemical reviews*, *108*(6), 2064-2110.

M. R. Rajan, M. Khousalya and R. Ramesh "Decontamination of Textile Dyeing Industry Effulent Using Iron Oxide Nanoparticles by Indian Journal of Applied Research"

Madden AS, Hochella MF Jr, Luxton TP (2006) Insights for size-dependent reactivity of hematite nanomineral surfaces through Cu2+ sorption. Geochimica et Cosmochimica Acta 70: 4095-4104

Modern Chemical Techniques, The Royal Society of Chemistry, 1998, pp. 92-115.

Mohammed Baalousha, 2008. Aggregation and disaggregation of iron oxide nanoparticles: Influence of particle concentration, pH and natural organic matter

Mohammed M. Rahman, Sher Bahadar Khan, Aslam Jamal, Mohd Faisal, and Abdullah M. Aisiri “Iron Oxide Nanoparticles by INTECH”, Kingdom of Saudi Arabia Link : http://cdn.intechopen.com/pdfs-wm/25341.pdf

Nigam, P., Banat, I. M., Singh, D., & Marchant, R. (1996). Microbial process for the decolorization of textile effluent containing azo, diazo and reactive dyes. *Process biochemistry, 31*(5), 435-442.

Niklaus Carter, The University of Maine “Physical Properties of Iron Oxide Nanoparticles”Link:http://digitalcommons.library.umaine.edu/cgi/viewcontent.cgi?article=12-05&context=honors

Nikulina, G.L., Deveikis, D.N and Pyshnov, G. 1995. Toxicity dynamics of anionic dyes in air of a work place and long term effects after absorption through skin. Med. Tr. Prom. Ekol., 6(25-28).

P.N. Srivastava and A. Prakash, “Bioaccumulation of heavy metals by algae and weath plants fed by textile effluents”, Journal of Industrial Pollution Control, vol. 7, pp. 25-30, 1991.

Pereira, L., & Alves, M. (2012). Dyes—environmental impact and remediation *Environmental protection strategies for sustainable development* (pp. 111-162): Springer.

Poedji Loekitowati Hariani., Muhammad Faizer., Ridwan Marsi and Dedi setiabudidaya.2013.Synthesis and properties of Fe3O4 Nanoparticles by Co-precipitation Methods to Removal procion Dye. International Journal of Environmental Science and Environment,4: 4046.

Premkumar, V., Rajan, M., & Ramesh, R. (2016). Removal of Toxic Substances From Textile Dyeing Industry Effluent Using Iron Oxide Nanoparticles. *PARIPEX-Indian Journal of Research, 5*(6).

S. Venturini and M. Tamaro, “Mutagenicity of anthraquinone and azo dyes in Ames Salmonella typhimurium test,” Mutation Research, vol. 68, pp. 307-312, 1979

Su, J.C. and Horton, J.J. 1998. Alergic contract dermatitis from azo dyes. Autralas. J. Dermatol., 39 (1) (48-49).

T. Shahwan, S.Abu Sirriah, M. Nairat, E. Boyaci, A.E. Eroglu, T.B. Scott, K.R. Hallam, 2011. Green synthesis of iron nanoparticles and their application as a Fenton-like catalyst for the degradation of aqueous cationic and anionic dyes.

Y. Hashimoto, H. Watanabe, and M. Degawa, “Mutagenicity of methoxyl derivatives of N-hydroxy-4- amino-azobenzenes and 4-nitroazobenzene,” Gann, vol. 68, pp. 373-374, 1977.

Y.H. Lin and J.Y. Leu, “Kinetics of reactive azo-dye decolorization by Pseudomonas luteola in a biological activated carbon process,” Biochemical Engineering Journal, vol. 39, pp. 457-467, 2008.